

Plasmonic interaction between nanospheres

S. Yu and H. Ammari

Research Report No. 2016-20

April 2016

Latest revision: April 2016

Seminar für Angewandte Mathematik
Eidgenössische Technische Hochschule
CH-8092 Zürich
Switzerland

PLASMONIC INTERACTION BETWEEN NANOSPHERES

SANGHYEON YU* AND HABIB AMMARI

ABSTRACT. When metallic nanospheres are nearly touching, strong nanofocusing of light can occur due to highly localized surface plasmons. It has potential applications in the design of nanophotonic devices, biosensing, and spectroscopy. Due to the singular behavior of electromagnetic fields in the narrow gap regions, its theoretical investigation is quite challenging in both analytical and numerical aspects. There are two approaches for studying the interaction between metallic spheres: transformation optics and the method of image charges. Here we clarify the connection between them. Based on the connection formula, we reveal the singular nature of plasmonic interaction between nanospheres in a completely analytical way. We also develop a hybrid numerical scheme for accurately and efficiently computing the field distribution produced by an arbitrary number of nearly touching plasmonic spheres.

Confining light at the nanoscale is challenging due to the diffraction limit. Strongly localized surface plasmon modes in singular metallic structures, such as two nearly touching surfaces, offer a promising route to overcome this difficulty.¹⁻⁶ Recently, Transformation Optics (TO) has been applied to analyze various structural singularities and then provides novel physical insights for a broadband nanofocusing of light.⁷⁻⁹ In particular, TO gives exact analytical solutions for 2D systems. However, there still remain several theoretical challenges for 3D case. Among 3D singular structures, the system of nearly touching spheres is of fundamental importance. Pendry et al.¹⁰ applied a TO inversion mapping to transform two spheres into a concentric shell and then provided a quasi-analytical solution which is an efficient numerical scheme. However, for a deeper theoretical understanding and practical purposes, a fully analytical description is still needed. Roughly speaking, the difficulty comes from the inhomogeneous material parameters in the transformed space.

Beside analytical obstacles, there are also numerical challenges. When the spheres are nearly touching, it requires a high computational cost to calculate the field enhancement accurately. The multipole expansion method requires a large number of moments and finite element method (or boundary element method) requires very fine mesh in the gap. Although the TO approach is efficient, it cannot be applied when the number of spheres is greater than two. So it is difficult to numerically investigate the collective resonant behavior such as Fano resonances.¹¹

In this article, we solve all these analytical and numerical challenges related to the singular nature of the plasmonic interaction between nearly touching spheres. The key of our approach is to clarify the connection between TO and the method of image charges. The principle of image method is to find fictitious sources which generate the desired reaction field. We derive a new explicit formula which can convert the image sources to TO-type solutions. Our second key ingredient is the image series solution for two dielectric spheres derived by Poladian.¹²⁻¹⁴ Since the image series is not convergent when the permittivity is negative, hence it cannot describe the plasmonic interaction. Our approach is to convert Poladian's solution into a TO-type series by using the connection formula, resulting in a fully analytical approximate solution valid for two plasmonic spheres. Our formula is highly accurate for a broad range of frequencies and gap distances.

For a cluster with an arbitrary number of spheres, Cheng and Greengard^{15, 16} developed a hybrid numerical scheme by combining the method of images and the multipole expansion method. Their scheme is extremely efficient and accurate even if the spheres are nearly touching. However, due to the non-convergence of the image series, their scheme needs to be modified for plasmonic spheres clusters. Again, by using the connection between TO and image sources, we develop a modified

(S.Y. and H.A.) DEPARTMENT OF MATHEMATICS, ETH ZÜRICH, RÄMISTRASSE 101, CH-8092 ZÜRICH, SWITZERLAND

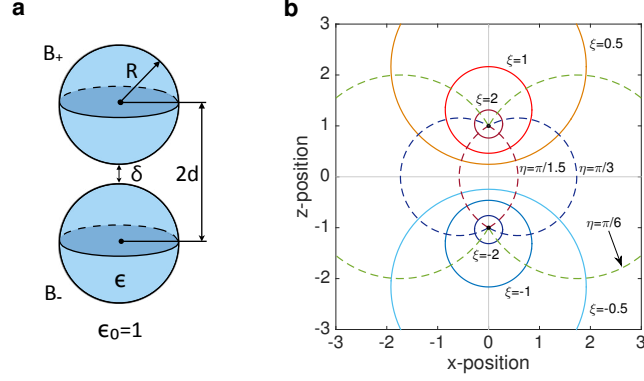


FIGURE 1. **Two spheres and the bispherical coordinates.** **a**, Two identical spheres, each of radius R and the permittivity ϵ , are separated by a distance δ . The distance between their centers is $2d$. The background permittivity is $\epsilon_0 = 1$. **b**, Coordinate level curves for the bispherical coordinate system with $\alpha = 1$. The solid lines (resp. the dashed lines) represent ξ (resp. η) coordinate curves.

hybrid scheme for an arbitrary configuration of plasmonic spheres clusters. We also show its extreme efficiency and accuracy by presenting several numerical examples. Our proposed scheme is a result of the interplay between three analytical approaches: TO, the image method, and the multipole expansion.

1. TRANSFORMATION OPTICS AND THE IMAGE METHOD

We consider the two metallic spheres described in Fig. 1a. The permittivity ϵ of each individual sphere is modeled as $\epsilon = 1 - \omega_p^2 / (\omega(\omega + i\gamma))$ where ω is the operating frequency, ω_p is the plasma frequency and γ is the damping parameter. We fit Palik's data for silver by adding a few Lorentz terms.¹⁷ We shall assume that the plasmonic spheres are small compared to optical wavelengths so that the quasi-static approximation can be adopted.

Let us briefly review the TO approach by Pendry et al.¹⁰ To transform two spheres into a concentric shell, Pendry et al. introduced the inversion transformation Φ defined as

$$\mathbf{r}' = \Phi(\mathbf{r}) = R_T^2 (\mathbf{r} - \mathbf{R}_0) / |\mathbf{r} - \mathbf{R}_0|^2 + \mathbf{R}'_0 \quad (1)$$

where $\mathbf{R}_0, \mathbf{R}'_0$ and R_T are given parameters. This inversion mapping induces the inhomogeneous permittivity $\epsilon'(\mathbf{r}') = R_T^2 |\mathbf{r}' - \mathbf{R}'_0| \epsilon$ in the transformed space. Then, by taking advantage of the symmetry of the shell, they represented the electric potential using $|\mathbf{r}' - \mathbf{R}'_0| (r')^{\pm(n+\frac{1}{2}) - \frac{1}{2}} Y_n^m(\theta', \phi')$ as basis functions. Here, $\{Y_n^m\}$ are the spherical harmonics.

The above TO description can be rewritten using the bispherical coordinates, (ξ, θ, φ) , as

$$e^{\xi - i\eta} = (z + i\rho + \alpha) / (z + i\rho - \alpha) \quad (2)$$

with $\rho = \sqrt{x^2 + y^2}$ and φ being the azimuthal angle.^{18,19} By letting $\mathbf{r}' = e^\xi (\sin \eta \cos \varphi, \sin \eta \sin \varphi, \cos \eta)$, $\mathbf{R}'_0 = (0, 0, 1)$, $\mathbf{R}_0 = (0, 0, \alpha)$ and $R_T^2 = 2\alpha$, we can see that the bispherical transformation is identical to the inversion mapping in the TO approach. In Fig. 1b, the geometry of the bispherical coordinates is described.

Any solution to the Laplace's equation can be represented as a sum of the following bispherical harmonics $\mathcal{M}_{n,\pm}^m(\mathbf{r})$:

$$\mathcal{M}_{n,\pm}^m(\mathbf{r}) = \sqrt{2} \sqrt{\cosh \xi - \cos \eta} e^{\pm(n+\frac{1}{2})\xi} Y_n^m(\eta, \varphi) \quad (3)$$

We will call $\mathcal{M}_{n,\pm}^m$ as TO basis since they are the same.

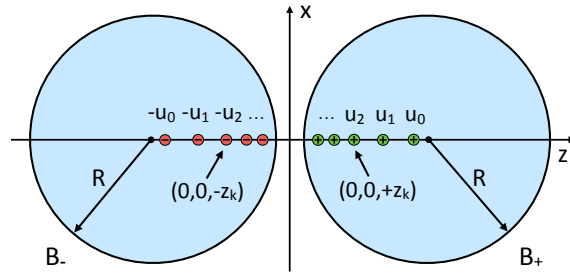


FIGURE 2. **Image charges for two spheres.** Red and green circles represent image charges placed along the z -axis.

Let us assume that two plasmonic spheres $B_+ \cup B_-$ are placed in a uniform incident field $(0, 0, E_0 \text{Re}\{e^{i\omega t}\})$. Then the quasi-static electric potential V outside the two spheres can be represented in the following form:

$$V(\mathbf{r}) = -E_0 z + \sum_{n=0}^{\infty} A_n (\mathcal{M}_{n,+}^0(\mathbf{r}) - \mathcal{M}_{n,-}^0(\mathbf{r})) \quad (4)$$

Here, the coefficients A_n satisfy some recurrence relations.²⁰ The TO approach also yields a similar tridiagonal system for A_n .¹⁰ Unfortunately, both of them cannot be solved analytically. The first goal in this article is to derive an approximate analytical expression for A_n by establishing the explicit connection between the method of images and TO.

Now we discuss the method of images. Since the imaging rule for a pair of cylinders is simple, an exact image series solution and its properties can be easily derived.^{21–25} However, for two dielectric spheres, an exact solution cannot be obtained due to the appearance of a continuous line image source.^{26–28} Poladian observed that the continuous source can be well approximated by a point charge and then derived an approximate but analytic image series solution.^{12–14} Let us briefly review Poladian's solution for two dielectric spheres. Let $\tau = (\epsilon - 1)/(\epsilon + 1)$, $s = \cosh^{-1}(d/R)$ and $\alpha = R \sinh s$. Suppose that two point charges of strength ± 1 are located at $(0, 0, \pm z_0) \in B_{\pm}$, respectively. By Poladian's imaging rule, they produce an infinite series of image charges of strength $\pm u_k$ at $(0, 0, \pm z_k)$ for $k = 0, 1, 2, \dots$, where z_k and u_k are given by

$$z_k = \alpha \coth(ks + s + t_0), \quad u_k = \tau^k \frac{\sinh(s + t_0)}{\sinh(ks + s + t_0)} \quad (5)$$

Here, the parameter t_0 is such that $z_0 = \alpha \coth(s + t_0)$. See Fig. 2. The potential $U(\mathbf{r})$ generated by all the above image charges is given by

$$U(\mathbf{r}) = \sum_{k=0}^{\infty} u_k (G(\mathbf{r} - \mathbf{z}_k) - G(\mathbf{r} + \mathbf{z}_k)) \quad (6)$$

where $\mathbf{z}_k = (0, 0, z_k)$ and $G(\mathbf{r}) = 1/(4\pi|\mathbf{r}|)$.

Let us consider the potential V outside the two spheres when a uniform incident field $(0, 0, E_0 \text{Re}\{e^{i\omega t}\})$ is applied. Let p_0 be the induced polarizability when a single sphere is subjected to the uniform incident field, that is, $p_0 = E_0 R^3 2\tau/(3 - \tau)$. Using the potential $U(\mathbf{r})$, we can derive an approximate solution for $V(\mathbf{r})$. For $|\tau| \approx 1$, we have

$$V(\mathbf{r}) \approx -E_0 z + 4\pi p_0 \left. \frac{\partial(U(\mathbf{r}))}{\partial z_0} \right|_{z_0=d} + QU(\mathbf{r})|_{z_0=d} \quad (7)$$

where Q is a constant chosen so that the right-hand side in equation (7) has no net flux on the surface of each sphere; see Supplementary Information for the derivation. The accuracy of the approximate formula, equation (7), improves as $|\epsilon|$ increases and it becomes exact when $|\epsilon| = \infty$. Moreover, its accuracy is pretty good even if the value of $|\epsilon|$ is moderate.

We now explain the difficulty in applying the the image series solution, equation (7), to the case of plasmonic spheres. In view of the expressions for u_k , equation (5), we can see that equation (7)

is not convergent when $|\tau| > e^s$. For plasmonic materials such as gold and silver, the real part of the permittivity ϵ is negative over the optical frequencies and then the corresponding parameter $|\tau|$ can attain any value in the interval (e^s, ∞) . Moreover, it turns out that all the plasmonic resonant values for τ are contained in the set $\{\tau \in \mathbb{C} : |\tau| > e^s\}$. So, equation (7) cannot describe the plasmonic interaction between the spheres due to the non-convergence.

2. CONNECTION FORMULA FROM IMAGE CHARGES TO TO

So far we have reviewed TO approach and the image method and pointed out their difficulties in solving the two plasmonic spheres problem. Now we clarify the connection between these two methods. We derive an explicit formula which converts the image charges to TO-type solutions as shown in the following lemma (see Supplementary Information for its proof).

Lemma 1. *(Converting image charges to TO) The potential $u_k G(\mathbf{r} \mp \mathbf{z}_k)$ generated by the image charge at $\pm \mathbf{z}_k$ can be rewritten using TO basis as follows: for $\mathbf{r} \in \mathbb{R}^3 \setminus (B_+ \cup B_-)$,*

$$u_k G(\mathbf{r} \mp \mathbf{z}_k) = \frac{\sinh(s + t_0)}{4\pi\alpha} \sum_{n=0}^{\infty} [\tau e^{-(2n+1)s}]^k e^{-(2n+1)(s+t_0)} \mathcal{M}_{n,\pm}^0(\mathbf{r}) \quad (8)$$

This identity plays a key role in our derivation of the approximate analytical solution. As mentioned previously, the reason why the image charge series, equation (6), does not work for plasmonic spheres is because the factor $(\tau e^{-s})^k$ may not converge to zero as $k \rightarrow \infty$. But the above connection formula helps us overcome this difficulty. If we sum up all the image charges in equation (8), we can see that the summation over k can be evaluated analytically using the following identity:

$$\sum_{k=0}^{\infty} [\tau e^{-(2n+1)s}]^k = \frac{e^{(2n+1)s}}{e^{(2n+1)s} - \tau} \quad (9)$$

Therefore, from equation (6) and Lemma 1, we obtain the following result.

Theorem 2. *(Converting image charge series to TO) Let $U(\mathbf{r})$ be defined as in equation (6). Then it can be rewritten using TO basis as follows: for $\mathbf{r} \in \mathbb{R}^3 \setminus (B_+ \cup B_-)$,*

$$U(\mathbf{r}) = \frac{\sinh(s + t_0)}{4\pi\alpha} \sum_{n=0}^{\infty} \frac{e^{-(2n+1)t_0}}{e^{(2n+1)s} - \tau} \left(\mathcal{M}_{n,+}^0(\mathbf{r}) - \mathcal{M}_{n,-}^0(\mathbf{r}) \right) \quad (10)$$

Clearly, the right-hand side of equation (10) does converge for any $|\tau| > e^s$ provided that $\tau \neq e^{(2n+1)s}$.

3. ANALYTICAL SOLUTION FOR TWO PLASMONIC SPHERES

Let us turn to the problem of two plasmonic spheres in an uniform incident field $(0, 0, E_0 \text{Re}\{e^{i\omega t}\})$. To derive the approximate analytical solution valid for two plasmonic spheres, we convert the image series solution, equation (7), into a TO-type solution by using the connection formula, equation (10). The result is shown in the following theorem (see Supplementary Information for its proof). We shall see that our analytical approximation completely captures the singular behavior of the exact solution.

Theorem 3. *If $|\tau| \approx 1$, the following approximation for the electric potential $V(\mathbf{r})$ holds: for $\mathbf{r} \in \mathbb{R}^3 \setminus (B_+ \cup B_-)$,*

$$V(\mathbf{r}) \approx -E_0 z + \sum_{n=0}^{\infty} \tilde{A}_n \left(\mathcal{M}_{n,+}^0(\mathbf{r}) - \mathcal{M}_{n,-}^0(\mathbf{r}) \right) \quad (11)$$

where the coefficient \tilde{A}_n is given by

$$\begin{aligned} \tilde{A}_n &= E_0 \frac{2\tau\alpha}{3 - \tau} \cdot \frac{2n + 1 - \gamma_0}{e^{(2n+1)s} - \tau} \\ \gamma_0 &= \sum_{n=0}^{\infty} \frac{2n + 1}{e^{(2n+1)s} - \tau} \bigg/ \sum_{n=0}^{\infty} \frac{1}{e^{(2n+1)s} - \tau} \end{aligned} \quad (12)$$

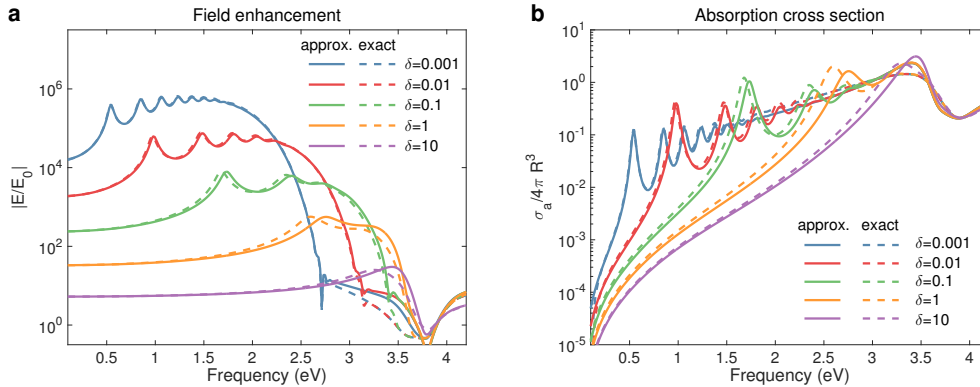


FIGURE 3. Exact solution vs Analytic approximation. **a**, Field enhancement plot as a function of frequency ω for various separation distances δ . The solid lines represent the approximate analytical solution and the dashed lines represent the exact solution. Two identical silver spheres of radius 30 nm are considered. **b**, Same as **a** but for the absorption cross section.

As expected, the above approximate expression is valid even if $|\tau| > e^s$. Therefore, it can furnish useful information about the plasmonic interaction between the two spheres. As a first demonstration, let us investigate the (approximate) resonance condition, that is, the condition for τ at which the coefficients \tilde{A}_n diverge. One might conclude that the resonance condition is given by $\tau = e^{(2n+1)s}$. However, one can see that \tilde{A}_n has a removable singularity at each $\tau = e^{(2n+1)s}$. In fact, the (approximate) resonance condition turns out to be

$$\sum_{n=0}^{\infty} \frac{1}{e^{(2n+1)s} - \tau} = 0 \quad (13)$$

In other words, the plasmonic resonance does happen when τ is one of zeros of equation (13). It turns out that the zeros $\{\tau_n\}_{n=0}^{\infty}$ lie on the positive real axis and satisfy, for $n = 0, 1, 2, \dots$,

$$e^{(2n+1)s} < \tau_n < e^{(2n+3)s} \quad (14)$$

The above estimate give us some insights into the asymptotic behavior of the resonance when two spheres get closer. As the separation distance δ goes to zero, the parameter s also goes to zero (in fact, $s = O(\delta^{1/2})$). Then, in view of equation (14), τ_n will converge to 1 and the corresponding permittivity ϵ_n goes to infinity. This means that a red-shift of the (bright) resonance modes does occur. Since the approximate analytical formula for V becomes more accurate as $|\epsilon|$ increases, we can expect that accuracy improves as the separation distance goes to zero. It indicates that the formula contains singular nature of the field distribution completely. Also, the difference between τ_n and τ_{n+1} decreases, which means that the spectrum becomes a nearly continuous one.

It is worth mentioning that the resonance condition, equation (13), is also interesting from a mathematical point of view. It is known that the plasmon resonance occurs when $1/(2\tau)$ is close to one of the eigenvalues of the Neumann-Poincaré operator.^{29–33} So equation (13) gives the approximate eigenvalues of the Neumann-Poincaré operator in the case of two spheres.

We now derive approximate formulas for the field at the gap and for the absorption cross section. From Theorem 3, we obtain the following (see Supplementary Information for the details):

$$E(0, 0, 0) \approx E_0 - E_0 \frac{8\tau}{3 - \tau} \left[\sum_{n=0}^{\infty} \frac{(2n+1)^2}{e^{(2n+1)s} - \tau} (-1)^n - \gamma_0 \sum_{n=0}^{\infty} \frac{2n+1}{e^{(2n+1)s} - \tau} (-1)^n \right] \quad (15)$$

In the quasi-static approximation, the absorption cross section σ_a is defined by $\sigma_a = \omega \text{Im}\{p\}$, where p is the polarizability of the system of two spheres. From Theorem 3, σ_a is approximated

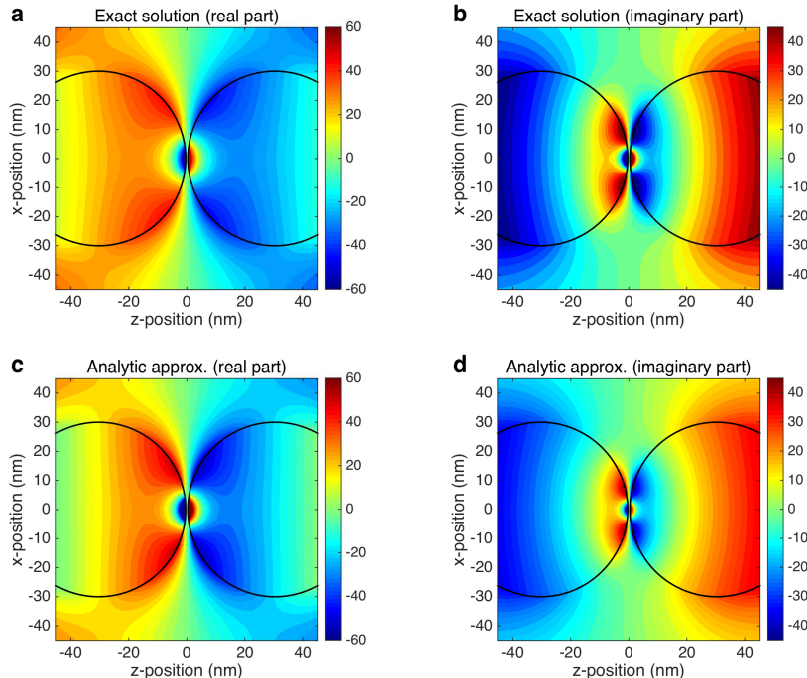


FIGURE 4. **Potential distributions for two identical silver spheres of radius 30 nm separated by $\delta = 0.25$ nm.** (a,b), Real and imaginary parts of the exact solution. The uniform incident field $(0, 0, \text{Re}\{e^{i\omega t}\})$ is applied at the frequency $\omega = 3.0$ eV in z -direction. (c,d), Same as (a,b) but for the analytical approximate solution.

as follows (see again Supplementary Information):

$$\sigma_a \approx \omega E_0 \frac{8\tau\alpha^3}{3-\tau} \left[\sum_{n=0}^{\infty} \frac{(2n+1)^2}{e^{(2n+1)s} - \tau} - \left(\sum_{n=0}^{\infty} \frac{2n+1}{e^{(2n+1)s} - \tau} \right)^2 / \sum_{n=0}^{\infty} \frac{1}{e^{(2n+1)s} - \tau} \right] \quad (16)$$

We compare the above approximate formulas with the exact ones. Fig. 3 represents respectively the field enhancement and the absorption cross section σ_a as functions of the frequency ω for various distances ranging from 0.001 nm to 10 nm. The good accuracy of our approximate formulas over broad ranges of frequencies and the gap distances is clearly shown. As mentioned previously, the accuracy improves as the spheres get closer. It is also worth highlighting the red-shift of the plasmon resonance modes as the separation distance δ goes to zero.^{3,34,35} In Fig. 4, we compare the exact and approximate electric potential distributions. They are also in good agreement and the field concentration in the gap region is observed.

4. HYBRID NUMERICAL SCHEME FOR MANY-SPHERES SYSTEM

Now we consider a system of an arbitrary number of plasmonic spheres. If all the spheres are well separated, then the multipole expansion method is efficient and accurate for computing the field distribution (see Supplementary Information). But, when the spheres are close to each other, the problem becomes very challenging since the charge densities on each sphere are nearly singular. To overcome this difficulty, Cheng and Greengard developed a hybrid numerical scheme combining the multipole expansion and the method of images.^{15,16} Their algorithm is extremely efficient and highly accurate even if the distance between the spheres is extremely small. However, due to non-convergence of the image series, their method cannot be applied to plasmonic spheres. The

second goal of this work is to show that the hybrid method can be extended to the system of plasmonic spheres by clarifying the connection between the method of images and TO.

The key ingredient in the hybrid method by Cheng and Greengard is the image source series produced by a general multipole source. Roughly speaking, Cheng and Greengard modified the multipole expansion method by replacing a multipole source with the image multipole potential. Let $\mathcal{Y}_{lm}(\mathbf{r})$ be a general multipole source, that is, $\mathcal{Y}_{lm}(\mathbf{r}) = Y_l^m(\theta, \phi)/r^{l+1}$. Suppose that a multipole source \mathcal{Y}_{lm} is located at the center of the sphere B_+ . Then the infinite sequence of the image sources is produced by Poladian's imaging rule. Let us denote the resulting potential by U_{lm}^+ . Similarly, let U_{lm}^- be the corresponding potential when the initial position is the center of B_- . The detailed image series representation for U_{lm}^\pm can be found in Supplementary Information. Again, the series are not convergent for $|\tau| > e^s$. Therefore, for extending Cheng and Greengard's method to the plasmonic case, it is essential to establish an explicit connection between the image multipole potential U_{lm}^\pm and TO. We derive the following formula for this connection (see Supplementary Information for its proof).

Theorem 4. (Converting image multipole series to TO) Assume that the integers l and m are such that $l \geq 1$ and $-l \leq m \leq l$. The potential U_{lm}^\pm can be rewritten in terms of TO basis as follows: for $\mathbf{r} \in \mathbb{R}^3 \setminus (B_+ \cup B_-)$,

$$\begin{aligned} U_{lm}^\pm(\mathbf{r}) &= \sum_{n=0}^{\infty} \frac{g_n^m \mathcal{D}_{lm}^\pm[\lambda_n^m]}{e^{2(2n+1)s} - \tau^2} (e^{(2n+1)s} \mathcal{M}_{n,\pm}^m(\mathbf{r}) - \tau \mathcal{M}_{n,\mp}^m(\mathbf{r})) \\ &\quad - \delta_{0m} \frac{\tilde{Q}_{l,1}^\pm}{2} \sum_{n=0}^{\infty} \frac{\mathcal{M}_{n,+}^0(\mathbf{r}) + (-1)^l \mathcal{M}_{n,-}^0(\mathbf{r})}{e^{(2n+1)s} + (-1)^l \tau} \\ &\quad \mp \delta_{0m} \frac{\tilde{Q}_{l,2}^\pm}{2} \sum_{n=0}^{\infty} \frac{\mathcal{M}_{n,+}^0(\mathbf{r}) - (-1)^l \mathcal{M}_{n,-}^0(\mathbf{r})}{e^{(2n+1)s} - (-1)^l \tau} \end{aligned} \quad (17)$$

where $g_n^m, \lambda_n^m, \mathcal{D}_{lm}^\pm$ and Q_l^\pm are given by

$$\begin{aligned} g_n^m &= \frac{1}{\alpha^{|m|+1}} \frac{2^{|m|}}{\sqrt{(2|m|)!}} \sqrt{\frac{(n+|m|)!}{(n-|m|)!}} \\ \lambda_n^m &= [\sinh(s+t_0)]^{2|m|+1} e^{-(2n+1)t_0} \\ N_{lm} &= (l-|m|)! \sqrt{\binom{l+|m|}{l+m}} \binom{l+|m|}{|m|+m} \\ \mathcal{D}_{lm}^\pm[f] &= \frac{(\pm 1)^{l-|m|}}{N_{lm}} \frac{\partial^{l-|m|}}{\partial [z_0(t_0)]^{l-|m|}} f \Big|_{z_0=d} \\ \tilde{Q}_{l,i}^\pm &= \sum_{n=0}^{\infty} \frac{(\pm 1)^l g_n^0 \mathcal{D}_{l0}^\pm[\lambda_n^0]}{e^{(2n+1)s} - (-1)^{l+i} \tau} \Big/ \sum_{n=0}^{\infty} \frac{1}{e^{(2n+1)s} - (-1)^{l+i} \tau} \end{aligned} \quad (18)$$

Here, δ_{lm} is the Kronecker delta.

Clearly, the above TO representation for U_{lm}^\pm does converge for $|\tau| > e^s$. Based on this, we develop a modified hybrid numerical scheme for the plasmonic spheres system. For a detailed description of the proposed scheme, we refer to Supplementary Information.

Next, we present numerical examples to illustrate the hybrid method. We consider two examples of the three-spheres configuration shown in Figs. 5a and 5d. We show comparison between multipole expansion method and the hybrid method by plotting the field enhancement at the gap center A . For the numerical implementation, only finite number of the multipoles \mathcal{Y}_{lm} or hybrid multipoles U_{lm}^\pm should be used. Let L be the truncation number for the order l . In Figs. 5b and 5e, the field enhancement is computed using the standard multipole expansion method. The computations give inaccurate results even if we include a large number of multipole sources with $L = 50$. On the contrary, the hybrid method gives pretty accurate results even for small values of

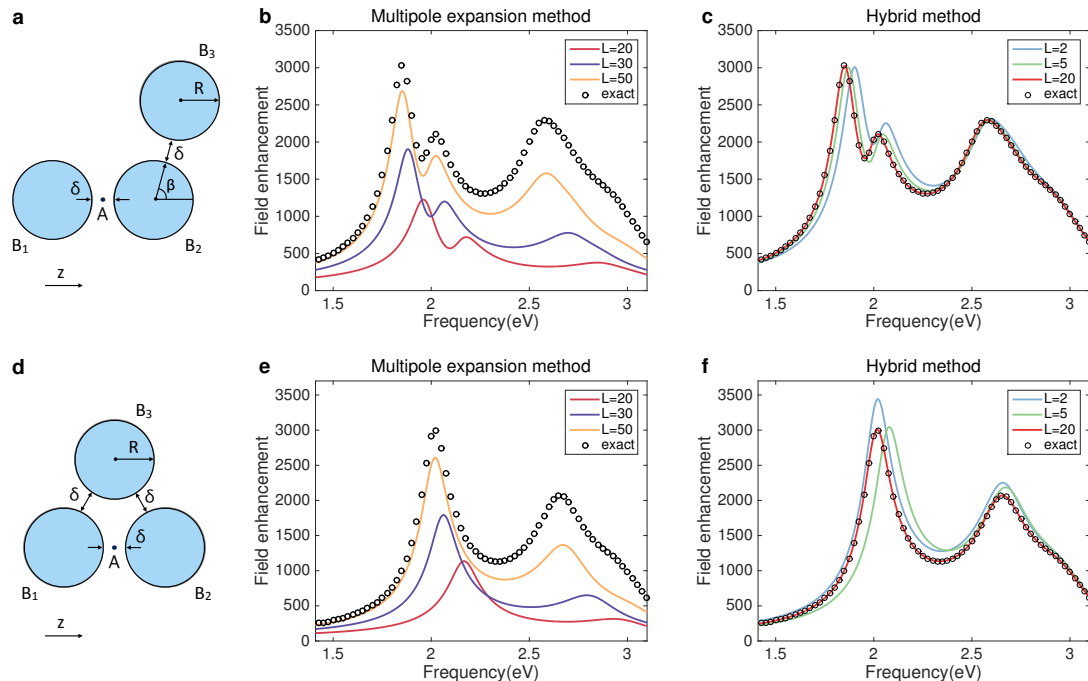


FIGURE 5. **Multipole expansion method vs Hybrid scheme.** **a,d**, Two examples of three spheres configuration. **b-c**, The field enhancement at point A as a function of frequency for the configuration **a** using the multipole expansion method and the hybrid method, respectively. The parameters are given as $R = 30$ nm, $\delta = 0.25$ nm and $\beta = 80^\circ$. **e-f**, Same as **b-c** but for the configuration **d**.

L such as $L = 2$ and 5 (Figs. 5c and 5f). Also, 99% accuracy can be achieved only with $L = 20$. For each hybrid multipole U_{lm}^\pm , the TO harmonics are included upto order $n = 300$ to ensure convergence and it can be evaluated very efficiently.

To achieve 99.9% accuracy at the first resonant peak, it is required to set $L = 150$ in the multipole expansion method and a $68,400 \times 68,400$ linear system needs to be solved. However, the same accuracy can be achieved only with $L = 23$ in the hybrid method. The corresponding linear system's size is $1,725 \times 1,725$ and it can be solved 2,000 times faster than that of the multipole expansion method. The reason for the extreme efficiency and accuracy is that the singular nature of the field distribution is already captured analytically in the hybrid multipole U_{lm}^\pm . In Fig. 6, we also show the field distribution for the three-spheres examples. The high field concentration in the narrow gap regions between nanospheres is clearly shown.

5. DISCUSSION

In this article we have fully characterized the singular behavior of nearly touching plasmonic nanospheres in an analytical way. We have derived an approximate analytical formula for the electric field for two plasmonic spheres. The formula is highly accurate for wide ranges of complex permittivities (or frequencies) and gap distances. Finally, we have extended Cheng and Greengard's hybrid numerical method to the case of plasmonic spheres. The extended scheme gives an extreme efficiency and accuracy for computing the field generated by an arbitrary number of plasmonic spheres. We have assumed that the spheres are identical only for simplicity. Our approach can be directly extended to the case where the spheres are not equisized and have different material parameters. A system of nanospheres on a plane (or a substrate) can also be considered. Moreover, by coupling with the fast multipole method, we expect that the proposed scheme will give an efficient numerical solver for a large scale problem.^{36,37} The nonlocal effect is an important issue

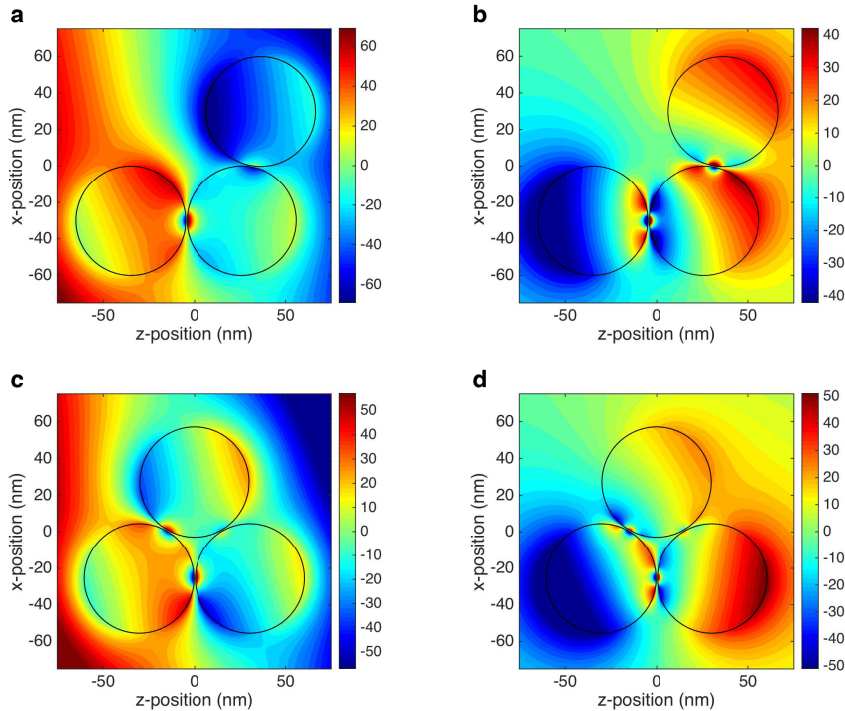


FIGURE 6. **Potential distributions for three spheres examples.** **a-b**, Real and imaginary parts of the potential for the configuration in Fig. 5a with $R = 30$ nm, $\delta = 0.25$ nm, and $\beta = 80^\circ$. The uniform incident field $(\sin 15^\circ, 0, \cos 15^\circ)\text{Re}\{e^{i\omega t}\}$ is applied at $\omega = 3.0$ eV. **c-d**, Same as **a-b** but for the configuration in Fig. 5d.

when the spheres are extremely closely spaced.^{38,39} By adopting the shifting boundary method developed by Luo et al.,³⁸ this effect can be easily incorporated.

Acknowledgments

The authors would like to thank Ross C. McPhedran and Graeme W. Milton for pointing out the existence of Poladian's thesis.¹²

Author contributions

All authors equally contributed to all aspects of the research.

Competing financial interests

The authors declare no competing financial interests.

Materials & Correspondence.

Correspondence and requests for materials should be addressed to S.Y. (sanghyeon.yu@sam.math.ethz.ch).

REFERENCES

- ¹ Gramotnev, D. K. & Bozhevolnyi, S. I. Plasmonics beyond the diffraction limit, *Nature Photonics* **4**, 83–91 (2010).
- ² Nordlander, P., Oubre, C., Prodan, E., Li, K. & Stockman, M. I. Plasmon hybridization in nanoparticle dimers. *Nano Lett.* **4**, 899–903 (2004).
- ³ Romero, I., Aizpurua, J., Bryant, G. W. & García de Abajo, F. J., Plasmons in nearly touching metallic nanoparticles: Singular response in the limit of touching dimers. *Opt. Express* **14**, 9988–9999 (2006).
- ⁴ Schuller, J. A. et al. Plasmonics for extreme light concentration and manipulation. *Nature Mater.* **9**, 193204 (2010).

- ⁵ Stockman, M. I. Nanofocusing of optical energy in tapered plasmonic waveguides. *Phys. Rev. Lett.* **93**, 137404 (2004).
- ⁶ Sweatlock, L. A., Maier, S. A., Atwater, H. A., Penninkhof, J. J. & Polman, A. Highly confined electromagnetic fields in arrays of strongly coupled Ag nanoparticles. *Phys. Rev. B* **71**, 235408 (2005).
- ⁷ Pendry, J. B., Luo, Y. & Zhao, R. Transforming the optical landscape. *Science* **348**, 521–524 (2015).
- ⁸ Pendry, J. B., Aubry, A., Smith, D. R. & Maier, S. A. Transformation optics and subwavelength control of light. *Science* **337**, 549–552 (2012).
- ⁹ Pendry, J. B., Schurig, D. & Smith, D. R. Controlling electromagnetic fields. *Science* **312**, 1780–1782 (2006).
- ¹⁰ Pendry, J. B., Fernández-Domínguez, A. I., Luo, Y. & Zhao, R. Capturing photons with transformation optics. *Nature Physics* **9**, 518–522 (2013).
- ¹¹ Luk'yanchuk, B. *et al.* The Fano resonance in plasmonic nanostructures and metamaterials. *Nature Materials* **9**, (2010) 707–715.
- ¹² Poladian, L. Effective Transport and Optical Properties of Composite Materials. Ph.D. thesis. (University of Sydney, 1990).
- ¹³ Poladian, L. General theory of electrical images in sphere pairs. *Q. J. Mech. Appl. Math.* **41**, 395–417 (1988).
- ¹⁴ Poladian, L. Asymptotic behaviour of the effective dielectric constants of composite materials. *Proc. Roy. Soc. A* **426**, 343–359 (1988).
- ¹⁵ Cheng, H. & Greengard, L. A method of images for the evaluation of electrostatic fields in systems of closely spaced conducting cylinders. *SIAM J. Appl. Math.* **58**, 121–141 (1998).
- ¹⁶ Cheng, H. On the method of images for systems of closely spaced conducting spheres. *SIAM J. Appl. Math.* **61**, 1324–1337 (2000).
- ¹⁷ Palik, E. D. *Handbook of Optical Constants of Solids* (Academic, 1985).
- ¹⁸ Smythe, W.R. *Static and Dynamic Electricity* (McGraw-Hill, New York, 1950).
- ¹⁹ Moon, P. & Spencer, D. E. *Field Theory Handbook. 2nd Ed.* (Springer-Verlag, Berlin, 1988).
- ²⁰ Goyette, A. & Navon, A. Two dielectric spheres in an electric field. *Phys. Rev. B* **13**, 4320–4327 (1976).
- ²¹ Ammari, H., Ciraolo, G., Kang, H., Lee, H. & Yun, K. Spectral analysis of the Neumann-Poincaré operator and characterization of the stress concentration in anti-plane elasticity. *Arch. Ration. Mech. Anal.* **208**, 275–304 (2013).
- ²² Ammari, H., Kang, H., Lee, H., Lee, J. & Lim, M. Optimal estimates for the electric field in two dimensions. *J. Math. Pures Appl.* **88**, 307–324 (2007).
- ²³ McPhedran, R. C. & Milton, G. W. Transport properties of touching cylinder pairs and of the square array of touching cylinders. *Proc. R. Soc. A* **411**, 313326 (1987).
- ²⁴ McPhedran, R. C., Poladian, L. & Milton, G. W. Asymptotic studies of closely spaced, highly conducting cylinders. *Proc. Roy. Soc. A* **415**, 185–196 (1988).
- ²⁵ Lim, M. & Yu, S., Asymptotics of the solution to the conductivity equation in the presence of adjacent circular inclusions with finite conductivities, *J. Math. Anal. Appl.* **421**, 131–156 (2015).
- ²⁶ Lindell, I. V. Electrostatic image theory for the dielectric sphere. *Radio Sci.* **27**, 1–8 (1992).
- ²⁷ Lindell, I. V., Sten, J. C.-E. & Nikoskinen, K. I. Electrostatic image method for the interaction of two dielectric spheres. *Radio Sci.* **28**, 319–329 (1993).
- ²⁸ Neumann, C. *Hydrodynamische Untersuchungen nebst einem Anhang uber die Probleme der Electrostatik und der magnetischen Induktion* pp. 279–282 (Teubner, Leipzig, 1883)
- ²⁹ Ammari, H., Deng, Y. & Millien, P. Surface plasmon resonance of nanoparticles and applications in imaging. *Arch. Ration. Mech. Anal.* **220**, 109–153 (2016).
- ³⁰ Ammari, H., Millien, P., Ruiz, M. & Zhang, H. Mathematical analysis of plasmonic nanoparticles: the scalar case. Preprint at <http://arxiv.org/abs/1506.00866> (2015).
- ³¹ Ammari, H., Ruiz, M., Yu, S. & Zhang, H. Mathematical analysis of plasmonic resonances for nanoparticles: the full Maxwell equations. Preprint at <http://arxiv.org/abs/1511.06817> (2015).
- ³² Ando, K. & Kang, H. Analysis of plasmon resonance on smooth domains using spectral properties of the Neumann-Poincaré operator. *J. Math. Anal. Appl.* **435**, 162–178 (2016).
- ³³ Khavinson, D., Putinar, M. & Shapiro, H. S. Poincaré’s variational problem in potential theory. *Arch. Ration. Mech. Anal.* **185**, 143–184 (2007).
- ³⁴ Schnitzer, O. Singular perturbations approach to localized surface-plasmon resonance: Nearly touching metal nanospheres. *Phys. Rev. B* **92**, 235428 (2015).
- ³⁵ Schnitzer, O., Giannini, V., Craster, R. V. & Maier, S. A. Asymptotics of surface-plasmon redshift saturation at subnanometric separations. *Phys. Rev. B* **93**, 041409 (2016).
- ³⁶ Greengard, L. & Rokhlin, V. A fast algorithm for particle simulations. *J. Comput. Phys.* **73**, 325–348 (1987).
- ³⁷ Greengard, L. & Rokhlin, V. On the numerical evaluation of electrostatic fields in dense random dispersions of cylinders. *J. Comput. Phys.* **136**, 629–639 (1997).
- ³⁸ Luo, Y., Zhao, R. & Pendry, J. B. van der Waals interactions at the nanoscale: The effects of nonlocality, *Proc. Natl. Acad. Sci. USA.* **111**, 18422–18427 (2014).
- ³⁹ Esteban, R., Borisov, A. G., Nordlander, P. & Aizpurua, J. Bridging quantum and classical plasmonics with a quantum-corrected model. *Nature Commun.* **3**, 825 (2012).

SUPPLEMENTARY INFORMATION FOR "PLASMONIC INTERACTION BETWEEN NANOSPHERES"

SANGHYEON YU AND HABIB AMMARI

The Supplementary Information (SI) is organized as follows. In section 1, we review the basics of the bispherical coordinates. In section 2, we collect various definitions and some of the properties of spherical harmonics. In section 3, we review Poladian's method of images for two dielectric spheres. In section 4, we prove our main result, which provides the connection between the Transformation Optics (TO) and the method of images. We also derive an approximate analytic solution for two plasmonic spheres in a uniform incident field. In section 5, we develop a hybrid numerical scheme for a system of arbitrary number of nearly touching plasmonic spheres. In section 6, we prove various useful formulas. For clarity and convenience, some parts of SI overlap with the main text.

1. BISPHERICAL COORDINATES (TO INVERSION MAPPING)

Here we review the definition and the properties of the bispherical coordinates. The bispherical coordinate system, (ξ, θ, φ) , is defined by

$$e^{\xi - i\theta} = (z + i\rho + \alpha)/(z + i\rho - \alpha) \quad (1)$$

where $\rho = \sqrt{x^2 + y^2}$, α is a positive constant and φ is the azimuthal angle measured from x -axis in the xy -plane. The Cartesian coordinates can be written in terms of the bispherical ones as follows:

$$x = \frac{\alpha \sin \eta \cos \varphi}{\cosh \xi - \cos \eta}, \quad y = \frac{\alpha \sin \eta \sin \varphi}{\cosh \xi - \cos \eta}, \quad z = \frac{\alpha \sinh \xi}{\cosh \xi - \cos \eta} \quad (2)$$

Note that the origin $(0, 0, 0)$ corresponds to $\xi = 0, \eta = \pi, \varphi = 0$. The point at infinity corresponds to $(\xi, \eta) \rightarrow (0, 0)$. On the other hand, it can be easily shown that the coordinate surfaces $\{\xi = c\}$ and $\{\theta = c\}$ for a nonzero c are respectively the zero level set of

$$\begin{aligned} f^\xi(x, y, z) &= (z - \alpha \coth c)^2 + \rho^2 - (\alpha/\sinh c)^2 \\ f^\eta(x, y, z) &= (\rho - \alpha \cot c)^2 + z^2 - (\alpha/\sin c)^2 \end{aligned} \quad (3)$$

Note also that the ξ -coordinate surface is the sphere of radius $\alpha/\sinh c$ centered at $(0, 0, \alpha \coth c)$. Therefore, $\xi = c$ (or $\xi = -c$) represents a sphere contained in the region $z > 0$ (resp. $z < 0$). Moreover, $|\xi| < c$ (resp. $|\xi| > c$) represents the region outside (resp. inside) the two spheres.

Suppose that two spheres B_+ and B_- of the same radius R are centered at $(0, 0, +d)$ and $(0, 0, -d)$, respectively. Let us parameterize the surfaces of these two spheres by $\{\xi = \pm s\}$. To do this, we set s and α by $d = \alpha \coth s$ and $R = \alpha \sinh s$ in view of equation (3). Note that $d = (\alpha/\sinh s) \cosh s = R \cosh s$.

It is well-known that any solution to the Laplace equation can be represented as a sum of the following bispherical harmonics $\mathcal{M}_{n,\pm}^m(\mathbf{r})$:

$$\mathcal{M}_{n,\pm}^m(\mathbf{r}) = \sqrt{2} \sqrt{\cosh \xi - \cos \eta} e^{\pm(n+\frac{1}{2})\xi} Y_n^m(\eta, \varphi) \quad (4)$$

(S.Y. and H.A.) DEPARTMENT OF MATHEMATICS, ETH ZÜRICH, RÄMISTRASSE 101, CH-8092 ZÜRICH, SWITZERLAND

The scale factors for the bispherical coordinates are

$$\sigma_\xi = \sigma_\eta = \frac{\alpha}{\cosh \xi - \cos \eta} \quad \text{and} \quad \sigma_\varphi = \frac{\alpha \sin \eta}{\cosh \xi - \cos \eta} \quad (5)$$

so that the gradient for scalar valued function g can be written in the form

$$\nabla g = \frac{1}{\sigma_\xi} \frac{\partial g}{\partial \xi} \mathbf{e}_\xi + \frac{1}{\sigma_\eta} \frac{\partial g}{\partial \eta} \mathbf{e}_\eta + \frac{1}{\sigma_\varphi} \frac{\partial g}{\partial \varphi} \mathbf{e}_\varphi \quad (6)$$

where $\{\mathbf{e}_\xi, \mathbf{e}_\eta, \mathbf{e}_\varphi\}$ is the unit basis vectors in the bispherical coordinates. The normal derivative on the surface $\{\xi = \pm s\}$ of the sphere B_\pm is given by

$$\frac{\partial}{\partial \mathbf{n}} \Big|_{\partial B_\pm} = \mp \mathbf{e}_\xi \cdot \nabla \Big|_{\partial B_\pm} = \mp \frac{\cosh s - \cos \eta}{\alpha} \frac{\partial}{\partial \xi} \Big|_{\xi=\pm s} \quad (7)$$

where \mathbf{n} denotes the outward unit normal vector.

If the function g is of the following form:

$$g(\mathbf{r}) = \sum_{n=0}^{\infty} \sum_{m=-n}^n c_n^m \mathcal{M}_{n,+}^m(\mathbf{r}) + d_n^m \mathcal{M}_{n,-}^m(\mathbf{r}) \quad (8)$$

then z -component of the gradient at the origin is given by

$$\mathbf{e}_z \cdot \nabla g(0, 0, 0) = \frac{2^{3/2}}{\alpha} \sum_{n=0}^{\infty} (c_n^0 - d_n^0)(n + 1/2)(-1)^n \quad (9)$$

where $\mathbf{e}_z = (0, 0, 1)$.

2. SOME DEFINITIONS AND PROPERTIES

- Let us define the spherical harmonics Y_l^m by

$$Y_{lm}(\theta, \phi) = \sqrt{\frac{(l-|m|)!}{(l+|m|)!}} P_l^{|m|}(\cos \theta) e^{im\phi} \quad (10)$$

where $P_l^m(x)$ is the associated Legendre polynomial given by

$$P_l^m(x) = (-1)^m (1-x^2)^{m/2} \frac{d^m}{dx^m} P_l(x) \quad (11)$$

Here, $P_l(x)$ is the Legendre polynomial of degree l .

- The Legendre polynomial $P_n(x)$ has the following generating function:

$$\frac{1}{\sqrt{1-2xt+t^2}} = \sum_{n=0}^{\infty} t^n P_n(x) \quad (12)$$

- The associated Legendre polynomial $P_n^m(x)$ has the following generating function:

$$(-1)^m (2m-1)!! \frac{(1-x^2)^{m/2} t^m}{[1-2xt+t^2]^{m+1/2}} = \sum_{n=0}^{\infty} t^n P_n^m(x) \quad (13)$$

- It holds that

$$P_n^n(x) = (-1)^n (2n-1)!! (1-x^2)^{n/2} \quad (14)$$

- Let us define the solid harmonics \mathcal{Y}_{lm} and \mathcal{Z}_{lm} by

$$\begin{aligned} \mathcal{Y}_{lm}(\mathbf{r}) &= r^{-(l+1)} Y_{lm}(\theta, \phi) \\ \mathcal{Z}_{lm}(\mathbf{r}) &= r^l Y_{lm}(\theta, \phi) \end{aligned} \quad (15)$$

The function \mathcal{Y}_{lm} is also called the multipole source.

- Let us introduce

$$w_{lm} = \begin{cases} 1, & m \geq 0 \\ (-1)^{|m|}, & m < 0 \end{cases} \quad (16)$$

- Let the constant N_{lmab} be given by

$$N_{lmab} = (-1)^{a+b} \sqrt{\binom{l+a-b+m}{l+m} \binom{l+a+b-m}{a+b}} \quad (17)$$

3. POLADIAN'S IMAGE METHOD FOR TWO SPHERES (REVIEW)

Here, we present a review of Poladian's image method for two dielectric spheres. First, we explain the image method when only a single sphere is placed in the whole space. Then we discuss an image series solution for two spheres in a uniform incident field. Finally, we consider the generalized image method for the case of multipole sources.

3.1. A single sphere. Suppose that a single sphere of radius R is centered at $(0, 0, 0)$. Let ϵ be the permittivity of the sphere. We also assume the background permittivity is $\epsilon_0 = 1$. Let $\tau = (\epsilon - 1)/(\epsilon + 1)$. When we locate a point charge Q at $(0, 0, c)$ with $c > R$, then it can be shown that the reaction potential is identical to the potential generated by the following two image sources:¹⁻³ (1) a point charge $Q' = -\tau(R/c)Q$ at $(0, 0, R^2/c)$ and (2) a continuous line source along the line segment from $(0, 0, 0)$ to $(0, 0, R^2/c)$ with a density function Λ given by

$$\Lambda(t) = \frac{\tau Q}{R(\epsilon + 1)} \left(\frac{R^2}{ct} \right)^{\frac{1}{2}(\tau+1)}, \quad t \in (0, R^2/c) \quad (18)$$

Poladian observed that the continuous line source can be well approximated by a point charge $-Q'$ at the center of the sphere $(0, 0, 0)$ provided that $|\epsilon|$ is large. In fact, this approximation becomes exact when $|\epsilon| = \infty$.

Therefore, Poladian's imaging rule for a single sphere can be summarized as follows: if a sphere of radius R is centered at $(0, 0, 0)$ and a point charge Q is located at $(0, 0, c)$, then the following two image charges are produced: (1) a point charge $Q' = -\tau(R/c)Q$ at $(0, 0, R^2/c)$ (2) a point charge $-Q'$ at the center of the sphere $(0, 0, 0)$.¹⁻³ Let us call the latter image charge *the neutralizing charge*.

3.2. Two spheres in a uniform field. Let us now consider the two spheres B_+ and B_- . Suppose that we locate a point charge of the magnitude ± 1 at the point $(0, 0, \pm z_0)$ in the sphere B_{\pm} , respectively. Due to the interaction between two spheres, an infinite sequence of image charges is generated along z -axis by Poladian's imaging rule. But it is difficult to keep track of all the image charges at each step of the recursive imaging process. Poladian found that it is much simpler to initially neglect the neutralizing charges and later introduce an additional image sources.

By ignoring the neutralizing charge in Poladian's imaging rule, we obtain an infinite sequence of the image charges as follows: for $m = 0, 1, 2, \dots$, m -th image charge $\pm u_m$ is located at the point $\pm \mathbf{z}_m = (0, 0, \pm z_m)$ in the sphere B_{\pm} , respectively, where z_m and u_m satisfy the following recursive relations:

$$d - z_{k+1} = \frac{R^2}{d + z_k}, \quad u_{k+1} = \tau \frac{R}{d + z_k} u_k \quad (19)$$

These recursive relations can be solved explicitly. To state the solutions for u_k and z_k , we introduce a parameter t_0 which satisfies

$$z_0 = \alpha \coth(s + t_0) \quad (20)$$

Note that if the initial position is equal to the center of each sphere (that is, $z_0 = d = R \cosh s$), then it holds that $t_0 = 0$. Using this representation for z_0 and the hyper-trigonometric identities, one can see that the solutions for z_k and u_k are given as follows:

$$\begin{aligned} z_k &= \alpha \coth(ks + s + t_0) \\ u_k &= \tau^k \frac{\sinh(s + t_0)}{\sinh(ks + s + t_0)} \end{aligned} \quad (21)$$

Let $G(\mathbf{r}) = 1/(4\pi|\mathbf{r}|)$ be the electric potential generated by a unit point charge. Then the potential $U(\mathbf{r})$ generated by all the above image charges is given by

$$U(\mathbf{r}) = \sum_{k=0}^{\infty} u_k (G(\mathbf{r} - \mathbf{z}_k) - G(\mathbf{r} + \mathbf{z}_k)) \quad (22)$$

where $\mathbf{z}_k = (0, 0, z_k)$.

Let us now consider the two spheres $B_+ \cup B_-$ placed in a uniform incident field. We assume the uniform field $(0, 0, E_0) \text{Re}\{e^{i\omega t}\}$ is applied where ω is the operating frequency. Let p_0 be the induced polarizability when a single sphere is subjected to the uniform incident field, that is, $p_0 = E_0 R^3 2\tau/(3 - \tau)$. We also let $D(\mathbf{r}) = \mathbf{e}_z \cdot \hat{\mathbf{r}}/(|\mathbf{r}|^2)$ be the potential generated by a point dipole source with a unit moment \mathbf{e}_z , where $\hat{\mathbf{r}} = \mathbf{r}/|\mathbf{r}|$. The uniform incident field is first imaged in each sphere, inducing an image point dipole source with the polarizability p_0 at the center of each sphere. Then these initial point dipoles produce an infinite sequence of image sources. The point dipole p_0 can be considered as the limit of two initial charges $\pm 4\pi p_0/2h$ at the points $z_0 = (0, 0, d \pm h)$ as $h \rightarrow 0$. It is equivalent to taking derivative $4\pi p_0 \partial/\partial z_0$ at $z_0 = d$. So we get the following expression for the image potential generated by the point dipole p_0 :¹⁻³

$$V_1(\mathbf{r}) := 4\pi p_0 \left. \frac{\partial(U(\mathbf{r}))}{\partial z_0} \right|_{z_0=d} \quad (23)$$

Using the following identity:

$$\left. \frac{\partial}{\partial z_0} \right|_{z_0=d} = - \frac{\sinh^2 s}{\alpha} \left. \frac{\partial}{\partial t_0} \right|_{t_0=0} \quad (24)$$

we can represent V_1 more explicitly in the form

$$\begin{aligned} V_1(\mathbf{r}) &= \sum_{m=0}^{\infty} p_m D(\mathbf{r} - \mathbf{r}_m) - q_m G(\mathbf{r} - \mathbf{r}_m) \\ &\quad + \sum_{m=0}^{\infty} p_m D(\mathbf{r} + \mathbf{r}_m) + q_m G(\mathbf{r} + \mathbf{r}_m) \end{aligned} \quad (25)$$

where \mathbf{r}_m, p_m and q_m are given by

$$\begin{aligned} \mathbf{r}_m &= \mathbf{z}_m|_{t_0=0} = (0, 0, \alpha \coth(m+1)s) \\ p_m &= \tau^m p_0 \left(\frac{\sinh s}{\sinh(m+1)s} \right)^3, \quad q_m = \tau^m \frac{p_0}{R} \frac{\sinh s \sinh ms}{\sinh^2(m+1)s} \end{aligned} \quad (26)$$

Note that $\pm \mathbf{r}_0$ is the center of the sphere B_{\pm} , respectively.

As pointed out by Poladian,¹ the potential V_1 is unphysical because the total charge on each sphere is non-zero. It originates from the fact that we have ignored the neutralizing image charges. Now we explain Poladian's strategy for neutralizing the total charge.¹ We introduce an additional potential by locating a point charge $\pm Q$ at the center of the sphere B_{\pm} , respectively. Then the corresponding image potential

is given by

$$\begin{aligned} V_2(\mathbf{r}) &:= QU(\mathbf{r})|_{z_0=d} \\ &= Q \sum_{m=0}^{\infty} u_m^0 (G(\mathbf{r} - \mathbf{r}_m) - G(\mathbf{r} + \mathbf{r}_m)) \end{aligned} \quad (27)$$

where u_k^0 is defined by

$$u_k^0 = u_k|_{t_0=0} = \tau^k \frac{\sinh s}{\sinh(k+1)s} \quad (28)$$

Now we choose the constant Q so that the potential $V_1 + V_2$ has no net flux on each sphere. Then Q becomes

$$Q = \sum_{j=0}^{\infty} q_j / \sum_{j=0}^{\infty} u_m^0 \quad (29)$$

Finally, we get the approximation for the potential $V(\mathbf{r})$ by superposing the uniform incident field and the aforementioned potentials:

$$V(\mathbf{r}) \approx -E_0 z + V_1(\mathbf{r}) + V_2(\mathbf{r}) \quad (30)$$

3.3. Image method for general multipole sources. We now consider the case when an initial image source is a multipole source \mathcal{Y}_{lm} . Note that, since the point charge potential G and the dipole potential D satisfy $G(\mathbf{r}) = \frac{1}{4\pi}\mathcal{Y}_{00}$ and $D(\mathbf{r}) = \mathcal{Y}_{10}(\mathbf{r})$, the image potentials, equations (22) and (23), can be seen as the special cases of potentials generated by the image multipole sources.

Before considering a general multipole source \mathcal{Y}_{lm} , let us first consider a sectoral multipole $\mathcal{Y}_{|m|,m}$. If an initial sectoral multipole $\mathcal{Y}_{|m|,m}$ is located at $(0, 0, z_0)$, the image sequence is produced by Poladian's rule¹⁻³ as follows: $u_m^{(2k)}\mathcal{Y}_{|m|,m}$ at $(0, 0, z_{2k})$ and $-u_m^{(2k+1)}\mathcal{Y}_{|m|,m}$ at $(0, 0, -z_{2k+1})$ for $k = 0, 1, 2, \dots$. Similarly, if an initial location is $(0, 0, -z_0)$, then the following image sequence is produced: $u_m^{(2k)}\mathcal{Y}_{|m|,m}$ at $(0, 0, -z_{2k})$ and $-u_m^{(2k+1)}\mathcal{Y}_{|m|,m}$ at $(0, 0, +z_{2k+1})$ for $k = 0, 1, 2, \dots$. Here, $u_m^{(k)}$ satisfies a recursive relation

$$u_m^{(k+1)} = \tau \left(\frac{R}{d + z_k} \right)^{2|m|+1} u_m^{(k)}, \quad k = 0, 1, 2, \dots \quad (31)$$

It can be explicitly solved as follows:

$$u_m^{(k)} = \tau^k \left(\frac{\sinh(s + t_0)}{\sinh(ks + s + t_0)} \right)^{2|m|+1} \quad (32)$$

Let U_m^\pm be the potential generated by the above image sequence when the initial sectoral multipole is located at $(0, 0, \pm z_0)$, respectively. Then the potential U_m^\pm is given by

$$U_m^\pm(\mathbf{r}) = \sum_{k=0}^{\infty} u_m^{(2k)}\mathcal{Y}_{|m|,m}(\mathbf{r} \mp \mathbf{z}_{2k}) - u_m^{(2k+1)}\mathcal{Y}_{|m|,m}(\mathbf{r} \pm \mathbf{z}_{2k+1}) \quad (33)$$

Let us turn to the case of a general multipole source $\mathcal{Y}_{lm}(\mathbf{r})$. Let U_{lm}^\pm be the potential due to the image sequence produced by an initial multipole source \mathcal{Y}_{lm} located at the center of the sphere B_\pm , respectively. It was shown that a general multipole source \mathcal{Y}_{lm} can be represented as a derivative of a sectoral multipole $\mathcal{Y}_{|m|,m}$:¹⁻³

$$\mathcal{Y}_{lm}(\mathbf{r} \mp \mathbf{r}_0) = \mathcal{D}_{lm}^\pm [\mathcal{Y}_{|m|,m}(\mathbf{r} \mp \mathbf{z}_0)] \quad (34)$$

where the differential operator \mathcal{D}_{lm}^\pm is defined by

$$\mathcal{D}_{lm}^\pm[f] = \frac{(\pm 1)^{l-|m|}}{(l-|m|)!N_{l,m,|m|,m}} \frac{\partial^{l-|m|}}{\partial z_0^{l-|m|}} f \Big|_{z_0=d} \quad (35)$$

Therefore, the image potential U_{lm}^\pm is also represented as a derivative of U_m^\pm as follows:

$$U_{lm}^\pm(\mathbf{r}) = \mathcal{D}_{lm}^\pm[U_m^\pm(\mathbf{r})] \quad (36)$$

Actually, this is not the end. We need to be careful when we consider the case when $m = 0$. In this case, the total charges on each sphere B_\pm may be non-zero. Since this is unphysical, we have to neutralize them again. We modify the potential U_{lm}^+ by adding an image potential produced by the following initial charges: a point charge $-Q_{l,1}^+$ (and $-Q_{l,2}^+$) at the center of the sphere B_+ (and B_-), respectively. We also modify the potential U_{lm}^- in a similar way with the initial charges $-Q_{l,i}^-$, $i = 1, 2$. Here, the constants $Q_{l,i}^\pm$ are chosen so that the total flux on each surface ∂B_\pm is zero. Specifically, the potential $U_{l,m}^\pm$ is modified as follows:

$$U_{lm}^\pm(\mathbf{r}) = \mathcal{D}_{lm}^\pm[U_m^\pm(\mathbf{r})] - \delta_{0m}Q_{l,1}^\pm U_0^+(\mathbf{r})|_{z_0=d} - \delta_{0m}Q_{l,2}^\pm U_0^-(\mathbf{r})|_{z_0=d} \quad (37)$$

where δ_{lm} is the Kronecker delta.

4. PROOFS: CONNECTION BETWEEN TO AND THE IMAGE METHOD & ANALYTICAL SOLUTION FOR TWO PLASMONIC SPHERES

Here, we present the proofs of our main results. First, we prove an explicit formula which connects the image method to TO. Then, using the connection formula, we derive an approximate analytic solution for two plasmonic spheres. We also discuss analytic expressions for the electric field at the gap center and the absorption cross section. Finally, we generalize the connection formula to the case of multipole sources.

4.1. Connection between image charges and TO. We prove the following connection formula which converts an image charge to a TO-type solution.

Lemma 1. (Connection formula for image charges) *The potential $u_k G(\mathbf{r} \mp \mathbf{z}_k)$ generated by the image charge can be rewritten using TO basis as follows: for $\mathbf{r} \in \mathbb{R}^3 \setminus (B_+ \cup B_-)$,*

$$u_k G(\mathbf{r} \mp \mathbf{z}_k) = \frac{\sinh(s+t_0)}{4\pi\alpha} \sum_{n=0}^{\infty} [\tau e^{-(2n+1)s}]^k \times e^{-(2n+1)(s+t_0)} \mathcal{M}_{n,\pm}^0(\mathbf{r}) \quad (38)$$

Proof. We have from equation (1) that

$$z + i\rho = \frac{2\alpha}{e^{\xi-i\eta} - 1} + \alpha \quad (39)$$

We also have the following identity:

$$\coth t = \frac{\sinh 2t}{\cosh 2t - 1} = \frac{2}{e^{2t} - 1} + 1 \quad (40)$$

Hence, by letting $\mathbf{z}(t) = (0, 0, \alpha \coth t)$, it follows that

$$\begin{aligned} \frac{1}{|\mathbf{r} - \mathbf{z}(t)|} &= |z + i\rho - \alpha \coth t|^{-1} \\ &= \frac{1}{2\alpha} \left| \frac{1}{e^{\xi-i\eta} - 1} - \frac{1}{e^{2t} - 1} \right|^{-1} \\ &= \frac{1}{2\alpha} \left| \frac{(e^{2t} - 1)(e^{\xi-i\theta} - 1)}{e^{2t}(e^{\xi-2t-i\theta} - 1)} \right|^{-1} \\ &= \frac{\sinh |t|}{\alpha} \frac{\sqrt{\cosh \xi - \cos \eta}}{\sqrt{\cosh(\xi - 2t) - \cos \eta}} \end{aligned} \quad (41)$$

From equation (12), it is easy to check that we have

$$\frac{1}{\sqrt{\cosh(\xi - 2t) - \cos \eta}} = \sqrt{2} \sum_{n=0}^{\infty} e^{-(n+\frac{1}{2})|\xi-2t|} P_n(\cos \theta) \quad (42)$$

Then, from equation (41), we get

$$\begin{aligned} \frac{\alpha}{\sinh |t|} \frac{1}{|\mathbf{r} \mp \mathbf{z}(t)|} &= \sqrt{2} \sqrt{\cosh \xi - \cos \theta} \\ &\times \sum_{n=0}^{\infty} e^{-(2n+1)t} e^{\pm(n+\frac{1}{2})\xi} P_n(\cos \theta) \end{aligned} \quad (43)$$

Therefore, from the fact that $\mathbf{z}_k = \mathbf{z}(ks + s + t_0)$ and the definitions of u_k, G and $\mathcal{M}_{n,\pm}^m$, the conclusion follows. \square

As explained in the main text, by applying the above lemma to equation (22) and using the identity

$$\sum_{k=0}^{\infty} [\tau e^{-(2n+1)s}]^k = \frac{e^{(2n+1)s}}{e^{(2n+1)s} - \tau} \quad (44)$$

we obtain the following connection formula which converts the image charge series U into a TO-type solution.

Theorem 2. (Converting the image charge series to TO) Let $U(\mathbf{r})$ be defined as in equation (22). Then $U(\mathbf{r})$ can be rewritten using TO basis as follows: for $\mathbf{r} \in \mathbb{R}^3 \setminus (B_+ \cup B_-)$,

$$U(\mathbf{r}) = \frac{\sinh(s + t_0)}{4\pi\alpha} \sum_{n=0}^{\infty} \frac{e^{-(2n+1)t_0}}{e^{(2n+1)s} - \tau} \left(\mathcal{M}_{n,+}^0(\mathbf{r}) - \mathcal{M}_{n,-}^0(\mathbf{r}) \right) \quad (45)$$

4.2. Analytical solution for two plasmonic spheres. We consider the two plasmonic spheres in a uniform incident field $(0, 0, E_0 \text{Re}\{e^{i\omega t}\})$. We derive an approximate analytical solution for the quasi-static electric potential V in the following theorem.

Theorem 3. If $|\tau| \approx 1$, the following approximation for the electric potential $V(\mathbf{r})$ holds: for $\mathbf{r} \in \mathbb{R}^3 \setminus (B_+ \cup B_-)$,

$$V(\mathbf{r}) \approx -E_0 z + \sum_{n=0}^{\infty} \tilde{A}_n (\mathcal{M}_{n,+}^0(\mathbf{r}) - \mathcal{M}_{n,-}^0(\mathbf{r})) \quad (46)$$

where the coefficient \tilde{A}_n is given by

$$\begin{aligned} \tilde{A}_n &= E_0 \frac{2\tau\alpha}{3 - \tau} \times \frac{2n + 1 - \gamma_0}{e^{(2n+1)s} - \tau} \\ \gamma_0 &= \sum_{n=0}^{\infty} \frac{2n + 1}{e^{(2n+1)s} - \tau} \bigg/ \sum_{n=0}^{\infty} \frac{1}{e^{(2n+1)s} - \tau} \end{aligned} \quad (47)$$

Proof. We shall prove the result by applying our connection formula to Poladian's image series solution. From Theorem 2 and the following identity:

$$\frac{\partial}{\partial z_0} \Big|_{z_0=d} = -\frac{\sinh^2 s}{\alpha} \frac{\partial}{\partial t_0} \Big|_{t_0=0} \quad (48)$$

we get

$$\begin{aligned} V_1(\mathbf{r}) &= 4\pi p_0 \partial_{z_0} \Big|_{z_0=d} U(\mathbf{r}) \\ &= E_0 \frac{2\tau\alpha}{3 - \tau} \sum_{n=0}^{\infty} \frac{2n + 1 - \coth s}{e^{(2n+1)s} - \tau} (\mathcal{M}_{n,+}^0(\mathbf{r}) - \mathcal{M}_{n,-}^0(\mathbf{r})) \end{aligned} \quad (49)$$

Similarly, we have

$$V_2(\mathbf{r}) = QU(\mathbf{r})|_{z_0=d} = Q \sum_{n=0}^{\infty} \frac{\mathcal{M}_{n,+}^0(\mathbf{r}) - \mathcal{M}_{n,-}^0(\mathbf{r})}{e^{(2n+1)s} - \tau} \quad (50)$$

Now let us consider the constant Q . The expression for Q in equation (29) does not converge when $|\tau| > e^s$. So, here we derive the constant Q in a slightly different way. We impose the following condition:

$$\int_{\partial B_+} \frac{\partial V_1}{\partial \mathbf{n}} dS + \int_{\partial B_+} \frac{\partial V_2}{\partial \mathbf{n}} dS = 0 \quad (51)$$

Then, by using Theorem 9, we obtain

$$E_0 \frac{2\tau\alpha}{3-\tau} \sum_{n=0}^{\infty} \frac{2n+1 - \coth s}{e^{(2n+1)s} - \tau} + Q \sum_{n=0}^{\infty} \frac{1}{e^{(2n+1)s} - \tau} = 0 \quad (52)$$

Hence, we see that

$$Q = -\gamma_0 + E_0 \frac{2\tau\alpha}{3-\tau} \coth s \quad (53)$$

Therefore, from equations (30), (49) and (50), the conclusion follows. \square

4.3. Electric field at the origin and the polarizability. From equation (9), we can see that the magnitude of the electric field at the gap is given by

$$E = -(\nabla V \cdot \mathbf{e}_z)(0, 0, 0) = E_0 - \frac{2^{3/2}}{\alpha} \sum_{n=0}^{\infty} A_n (2n+1) (-1)^n \quad (54)$$

As mentioned in the main text, the absorption cross section σ_a is given by $\sigma_a = \omega \text{Im}\{p\}$ where p is the polarizability. It was shown that the polarizability p is given by⁴

$$p = \sqrt{2}\alpha^2 \sum_{n=0}^{\infty} (2n+1) A_n \quad (55)$$

Therefore, by replacing A_n by \tilde{A}_n , we can derive approximate analytical expressions for E and σ_a .

4.4. Connection formula for general multipole sources. Here we generalize our connection formula to the case of general multipole sources $\mathcal{Y}_{lm}(\mathbf{r})$. As mentioned in the main text, it is essentially used to develop a hybrid numerical scheme for plasmonic spheres clusters.

We first consider the sectoral multipole $\mathcal{Y}_{|m|,m}$. We can represent the potential $u_m^{(k)} \mathcal{Y}_{|m|,m}(\mathbf{r} \mp \mathbf{z}_k)$ using TO basis as follows.

Lemma 4. (Converting image sectoral multipole to TO) For $\mathbf{r} \in \mathbb{R}^3 \setminus (B_+ \cup B_-)$, we have

$$u_m^{(k)} \mathcal{Y}_{|m|,m}(\mathbf{r} \mp \mathbf{z}_k) = \sum_{n=|m|}^{\infty} g_n^m \lambda_n^m [\tau e^{-(2n+1)s}]^k \times e^{-(2n+1)s} \mathcal{M}_{n,\pm}^m(\mathbf{r}) \quad (56)$$

where λ_n^m and g_n^m are given by

$$\begin{aligned} \lambda_n^m &= [\sinh(s+t_0)]^{2|m|+1} e^{-(2n+1)t_0} \\ g_n^m &= \frac{1}{\alpha^{|m|+1}} \frac{2^{|m|}}{\sqrt{(2|m|)!}} \sqrt{\frac{(n+|m|)!}{(n-|m|)!}} \end{aligned} \quad (57)$$

Proof. For simplicity, we consider only $u_m^{(k)} \mathcal{Y}_{|m|,m}(\mathbf{r} - \mathbf{z}_k)$. From equation (14) and the fact that $\rho = |\mathbf{r} - \mathbf{z}_k| \sin \theta_k$, we have

$$\begin{aligned} \mathcal{Y}_{|m|,m}(\mathbf{r} - \mathbf{z}_k) &= \frac{1}{\sqrt{(2|m|)!}} \frac{P_{|m|}^{(|m|)}(\cos \theta_k) e^{im\phi_k}}{|\mathbf{r} - \mathbf{z}_k|^{|m|+1}} \\ &= \omega_m \frac{[\sin \theta_k]^{|m|}}{|\mathbf{r} - \mathbf{z}_k|^{|m|+1}} e^{im\phi_k} \\ &= \omega_m \frac{\rho^{|m|}}{|\mathbf{r} - \mathbf{z}_k|^{2|m|+1}} e^{im\phi_k} \end{aligned} \quad (58)$$

where the constant ω_m is defined by

$$\omega_m = \frac{(-1)^{|m|} (2|m| - 1)!!}{\sqrt{(2|m|)!}} \quad (59)$$

From equation (41) and the fact that $\mathbf{z}_k = \mathbf{z}(ks + s + t_0)$, we see that

$$\frac{1}{|\mathbf{r} \mp \mathbf{z}_k|} = \frac{\sin(ks + s + t_0) \sqrt{\cosh \xi - \cos \eta}}{\alpha \sqrt{\cosh(\xi \mp 2(ks + s + t_0)) - \cos \eta}} \quad (60)$$

We also have from equation (2) that $\rho = \alpha \sin \eta / (\cosh \xi - \cos \eta)$. By substituting these expressions for $1/|\mathbf{r} - \mathbf{z}_k|$ and ρ into equation (58), we get

$$\begin{aligned} u_m^{(k)} \mathcal{Y}_{|m|,m}(\mathbf{r} - \mathbf{z}_k) &= \tau^k \frac{\sinh^{2|m|+1}(s + t_0)}{\sqrt{(2|m|)!} \alpha^{|m|+1}} \sqrt{\cosh \xi - \cos \eta} \\ &\quad \times \frac{2^{|m|+1/2} (-1)^{|m|} (2|m| - 1)!! [\sin \eta]^{|m|}}{[2(\cosh(\xi - 2(ks + s + t_0)) - \cos \eta)]^{|m|+1/2}} \end{aligned} \quad (61)$$

By letting $t = e^{-|\zeta|}$ and $x = \cos \eta$ in equation (13), it is easy to check that

$$\frac{(-1)^m (2m - 1)!! [\sin \eta]^m}{[2(\cosh \zeta - \cos \eta)]^{m+1/2}} = \sum_{n=m}^{\infty} e^{-(n+\frac{1}{2})|\zeta|} P_n^m(\cos \eta) \quad (62)$$

By applying this identity to equation (61), we immediately obtain that

$$\begin{aligned} u_m^{(k)} \mathcal{Y}_{|m|,m}(\mathbf{r} - \mathbf{z}_k) &= \tau^k 2^{|m|} \frac{\sinh^{2|m|+1}(s + t_0)}{\sqrt{(2|m|)!} \alpha^{|m|+1}} \\ &\quad \times \sqrt{2} \sqrt{\cosh \xi - \cos \eta} \\ &\quad \times \sum_{n=|m|}^{\infty} e^{-(2n+1)(ks+s+t_0)} e^{(n+\frac{1}{2})\xi} P_n^{|m|}(\cos \eta) \end{aligned} \quad (63)$$

for $|\zeta| < s$. Then, from the definition of $\mathcal{M}_{n,+}^m$, the conclusion follows. \square

Now we prove the generalized connection formula which converts the image multipole series U_{lm}^\pm to a TO-type solution.

Theorem 5. (Converting image multipole series to TO) Assume l and m are integers such that $l \geq 1$ and $-l \leq m \leq l$. Then the potential U_{lm}^\pm can be rewritten in terms of TO basis as follows: for $\mathbf{r} \in \mathbb{R}^3 \setminus (B_+ \cup B_-)$,

$$\begin{aligned} U_{lm}^\pm(\mathbf{r}) &= \sum_{n=|m|}^{\infty} \frac{g_n^m \mathcal{D}_{lm}^\pm[\lambda_n^m]}{e^{2(2n+1)s} - \tau^2} (e^{(2n+1)s} \mathcal{M}_{n,\pm}^m(\mathbf{r}) - \tau \mathcal{M}_{n,\mp}^m(\mathbf{r})) \\ &\quad - \delta_{0m} \frac{\tilde{Q}_{l,1}^\pm}{2} \sum_{n=0}^{\infty} \frac{\mathcal{M}_{n,+}^0(\mathbf{r}) + (-1)^l \mathcal{M}_{n,-}^0(\mathbf{r})}{e^{(2n+1)s} + (-1)^l \tau} \\ &\quad \mp \delta_{0m} \frac{\tilde{Q}_{l,2}^\pm}{2} \sum_{n=0}^{\infty} \frac{\mathcal{M}_{n,+}^0(\mathbf{r}) - (-1)^l \mathcal{M}_{n,-}^0(\mathbf{r})}{e^{(2n+1)s} - (-1)^l \tau} \end{aligned} \quad (64)$$

where the constants $\tilde{Q}_{l,i}^\pm$ are given by

$$\tilde{Q}_{l,i}^\pm = \sum_{n=0}^{\infty} \frac{(\pm 1)^l g_n^0 \mathcal{D}_{l0}^\pm[\lambda_n^0]}{e^{(2n+1)s} - (-1)^{l+i} \tau} \bigg/ \sum_{n=0}^{\infty} \frac{1}{e^{(2n+1)s} - (-1)^{l+i} \tau} \quad (65)$$

Proof. By applying Lemma 4 to equation (33) and then using the following identity:

$$\sum_{k=0}^{\infty} [\tau e^{-(2n+1)s}]^{2k} = \frac{e^{2(2n+1)s}}{e^{2(2n+1)s} - \tau^2} \quad (66)$$

we obtain

$$U_m^\pm(\mathbf{r}) = \sum_{n=|m|}^{\infty} g_n^m \lambda_n^m \frac{e^{(2n+1)s} \mathcal{M}_{n,\pm}^m(\mathbf{r}) - \tau \mathcal{M}_{n,\mp}^m(\mathbf{r})}{e^{2(2n+1)s} - \tau^2} \quad (67)$$

Then, by using equation (37), we get

$$\begin{aligned} U_{l,m}^\pm(\mathbf{r}) &= \sum_{n=|m|}^{\infty} \frac{g_n^m \mathcal{D}_{lm}^\pm[\lambda_n^m]}{e^{2(2n+1)s} - \tau^2} (e^{(2n+1)s} \mathcal{M}_{n,\pm}^m(\mathbf{r}) - \tau \mathcal{M}_{n,\mp}^m(\mathbf{r})) \\ &\quad - \delta_{0m} Q_{l,1}^\pm \frac{\sinh s}{\alpha} \sum_{n=0}^{\infty} \frac{e^{(2n+1)s} \mathcal{M}_{n,+}^0(\mathbf{r}) - \tau \mathcal{M}_{n,-}^0(\mathbf{r})}{e^{2(2n+1)s} - \tau^2} \\ &\quad - \delta_{0m} Q_{l,2}^\pm \frac{\sinh s}{\alpha} \sum_{n=0}^{\infty} \frac{(-\tau) \mathcal{M}_{n,+}^0(\mathbf{r}) + e^{(2n+1)s} \mathcal{M}_{n,-}^0(\mathbf{r})}{e^{2(2n+1)s} - \tau^2} \end{aligned} \quad (68)$$

Now we consider the following flux conditions:

$$\int_{\partial B_+} \frac{\partial(U_{l,m}^\pm)}{\partial \mathbf{n}} dS = 0, \quad \int_{\partial B_-} \frac{\partial(U_{l,m}^\pm)}{\partial \mathbf{n}} dS = 0 \quad (69)$$

Then, by applying Theorem 9 to the above conditions with equation (68), we obtain

$$Q_{l,1}^\pm \frac{\sinh s}{\alpha} = \frac{\tilde{Q}_{l,1}^\pm \pm \tilde{Q}_{l,2}^\pm}{2}, \quad Q_{l,2}^\pm \frac{\sinh s}{\alpha} = (-1)^l \frac{\tilde{Q}_{l,1}^\pm \mp \tilde{Q}_{l,2}^\pm}{2} \quad (70)$$

By rearranging the terms, the conclusion follows. \square

It is worth to remark that we can evaluate the derivatives $\mathcal{D}_{lm}^\pm[\lambda_n^m]$ analytically by using the Faà di Bruno's formula (we omit the details). Moreover, its numerical computation can be done efficiently using a recursive relation for Bell polynomials.

5. HYBRID NUMERICAL SCHEME FOR MANY PLASMONIC SPHERES

As mentioned in the main text, the numerical computation of the field generated by a system of spheres becomes quite challenging when the spheres are nearly touching. To overcome the difficulty, Cheng and Greengard developed a hybrid numerical scheme combining the multipole expansion and the method of images.^{5,6} But their scheme cannot be used when the spheres are plasmonic due to the non-convergence of the image series. Here, we present a brief review of the multipole expansion method and the hybrid numerical scheme developed by Cheng and Greengard^{5,6} and then explain their difficulties. Finally, we show that the Cheng and Greengard's hybrid method can be extended to the case of plasmonic spheres by using the connection between TO and the image method.

5.1. Multipole expansion. Suppose that the spheres $B_j, j = 1, 2, \dots, J$ of radius R are located disjointly in \mathbb{R}^3 and let \mathbf{c}_j be the center of the sphere B_j . We also suppose that all the spheres have the same permittivity ϵ and the background permittivity is given as $\epsilon_0 = 1$. The classical way to solve the many-spheres problem is Rayleigh's multipole expansion method. Here, we briefly review this method. Recall that the solid harmonics \mathcal{Y}_{lm} and \mathcal{Z}_{lm} are defined by

$$\mathcal{Y}_{lm}(\mathbf{r}) = \frac{Y_l^m(\theta, \phi)}{r^{l+1}}, \quad \mathcal{Z}_{lm}(\mathbf{r}) = r^l Y_l^m(\theta, \phi) \quad (71)$$

Any solution to Laplace's equation can be represented as a sum of \mathcal{Y}_{lm} and \mathcal{Z}_{lm} . The potential $V(\mathbf{r})$ can be represented as the following multipole expansion: for \mathbf{r} belonging to the region outside the spheres, we have

$$V(\mathbf{r}) = -E_0 z + \sum_{j=1}^J \sum_{l=1}^{\infty} \sum_{m=-l}^l C_{j,lm} \mathcal{Y}_{lm}(\mathbf{r} - \mathbf{c}_j) \quad (72)$$

where the coefficients $C_{j,lm}$ are unknown constants. For the inner region of B_j , we can easily extend the above representation by imposing the continuity of the potential on the surface ∂B_j . For $\mathbf{r} \in B_j$, we have

$$V(\mathbf{r}) = \sum_{l=0}^{\infty} \sum_{m=-l}^l C_{j,lm} \frac{\mathcal{Z}_{lm}(\mathbf{r} - \mathbf{c}_j)}{R^{2l+1}} \quad (73)$$

Then, by using the addition formula for solid harmonics (see equation (85)) and the flux boundary conditions, $\nabla V \cdot \mathbf{n}|_{ext} = \epsilon \nabla V \cdot \mathbf{n}|_{int}$ on the surface ∂B_j , the infinite dimensional linear system for unknowns $C_{j,lm}$ can be derived. If all the spheres are well-separated, good accuracy can be achieved by truncating the linear system by a small order. But, if some of the spheres are close to touching, the charge densities on their surfaces become nearly singular. So more harmonics are required to describe them accurately.

5.2. Cheng and Greengard's hybrid method. To illustrate the hybrid method by Cheng and Greengard,^{5,6} let us consider an example of three spheres (that is, $J = 3$). Suppose that the spheres B_1 and B_2 are closely located but well-separated from B_3 . Then the charge density on ∂B_3 can be well represented by a low-order spherical harmonics expansion. But the charge densities both on ∂B_1 and ∂B_2 may be singular, so it is better to use the image method to describe their associated potentials. In view of this observation, Cheng and Greengard introduced the modified representation as

follows: for \mathbf{r} belongs to the region outside the spheres,

$$\begin{aligned}
 V(\mathbf{r}) = & -E_0z + \sum_{j=1}^2 \sum_{l=1}^{\infty} \sum_{m=-l}^l C_{12,lm} U_{12,lm}(\mathbf{r}) \\
 & + \sum_{l=1}^{\infty} \sum_{m=-l}^l C_{3,lm} \mathcal{Y}_{lm}(\mathbf{r} - \mathbf{c}_3)
 \end{aligned} \tag{74}$$

where $U_{12,lm}$ is the image series solution which includes all the image sources induced from the multipoles $C_{j,lm} \mathcal{Y}_{lm}(\mathbf{r} - \mathbf{c}_j)$, $j = 1, 2$, by the interaction between two spheres B_1 and B_2 .^{5,6} This representation for $V(\mathbf{r})$ can be directly generalized to a system of an arbitrary number of spheres. The resulting scheme is extremely efficient and accurate even if the spheres are nearly touching. This is because the close-to-touching interaction is already captured in the image multipole series. However, the image method cannot be applied for plasmonic spheres due to the non-convergence. So, our strategy for extending the hybrid method to the case of plasmonic spheres is to convert the image multipole series to a TO-type solution.

5.3. Outline of the modified algorithm. Using the connection between TO and the image multipole potential U_{lm}^{\pm} (Theorem 5), we develop the modified hybrid numerical scheme for a system of plasmonic spheres. Here, we present the outline of the algorithm of our proposed scheme.

- 1 Write down the potential $V(\mathbf{r})$ in the multipole expansion form as in equation (72).
- 2 If a pair of spheres, say B_j and B_k , are closely located (if the separation distance is smaller than a given number, for example, the radius R), then we rotate the xyz -axis for both $\mathbf{r} - \mathbf{c}_j$ and $\mathbf{r} - \mathbf{c}_k$ so that the $+z$ -axis is in the direction of the axis of the pair of spheres, that is, $\mathbf{c}_j - \mathbf{c}_k$.
- 3 We also transform the multipole expansion for B_j into the rotated frame using equation (86). Let us denote the coefficients in the rotated frame by $C'_{j,lm}$.
- 4 By using the connection formula for general multipoles (Theorem 5), we modify the multipole expansion in the rotated frame by replacing $C'_{j,lm} \mathcal{Y}_{lm}(\mathbf{r})$ with the hybrid TO multipole $C'_{j,lm} U_{lm}^+(\mathbf{r})$.
- 5 Do the same as in step 4 for B_k with $U_{lm}^-(\mathbf{r})$ instead of $U_{lm}^+(\mathbf{r})$.
- 6 We convert the TO-type expansion for B_j and B_k into the form of multipole expansion using Theorem 8.
- 7 Rotate the axis of the coordinate system and transform the multipole expansions into the original frame.
- 8 Perform steps 2-7 for all the pairs of closely spaced spheres.
- 9 We extend the resulting multipole expansion to the inner regions of B_j for $j = 1, 2, \dots, J$ using Theorem 7.
- 10 By applying the addition formula, equation (85), for \mathcal{Y}_{lm} and \mathcal{Z}_{lm} with the flux boundary conditions, we construct the infinite dimensional linear system for unknowns $C_{j,lm}$.
- 11 We solve the linear system after a truncation.

6. USEFUL FORMULAS

Here we collect many useful formulas and give their proofs.

6.1. Potential inside two spheres. The following theorems are useful for finding a potential inside the two spheres when we have an explicit representation of the potential in the outside region.

Theorem 6. Suppose that V satisfies the Laplace equation inside and outside the two spheres B_+ and B_- . We also assume that the potential V is continuous on each surface ∂B_\pm . We also assume that, outside the spheres, the potential V is given by

$$V(\mathbf{r}) = \sum_{n=0}^{\infty} \sum_{m=-n}^n a_{n,+}^m \mathcal{M}_{n,+}^m(\mathbf{r}) + a_{n,-}^m \mathcal{M}_{n,-}^m(\mathbf{r}) \quad (75)$$

for $\mathbf{r} \in \mathbb{R}^3 \setminus (B_+ \cup B_-)$ and some coefficients $a_{n,\pm}^m$. Then, inside the spheres, the potential $V(\mathbf{r})$ for $\mathbf{r} \in B_\pm$ is given by

$$V(\mathbf{r}) = \sum_{n=0}^{\infty} \sum_{m=-n}^n (a_{n,\pm}^m e^{(2n+1)s} + a_{n,\mp}^m) \mathcal{M}_{n,\mp}^m(\mathbf{r}) \quad (76)$$

Proof. It is obvious that the series on the right-hand side satisfies the Laplace equation. Since $\partial B_\pm = \{\xi = \pm s\}$, we have the following identity:

$$\begin{aligned} \mathcal{M}_{n,+}^m(\mathbf{r})|_{\partial B_\pm} &= \sqrt{2} \sqrt{\cosh \xi - \cos \eta} e^{\pm(n+1/2)s} Y_n^m(\eta, \varphi) \\ &= e^{\pm(2n+1)s} \mathcal{M}_{n,-}^m(\mathbf{r})|_{\partial B_\pm} \end{aligned} \quad (77)$$

Then one can easily check that the potential V is continuous on each surface $\partial B_\pm = \{\xi = \pm s\}$. Therefore, the proof is completed. \square

Theorem 7. Suppose that V satisfies the Laplace equation inside and outside the two spheres B_+ and B_- . We also assume that the potential V is continuous on each surface ∂B_\pm . Furthermore, we assume that, outside the spheres, the potential V is given by

$$V(\mathbf{r}) = \sum_{l=0}^{\infty} \sum_{m=-l}^l f_{lm}^+ \mathcal{Y}_{lm}(\mathbf{r} - \mathbf{r}_0) + f_{lm}^- \mathcal{Y}_{lm}(\mathbf{r} + \mathbf{r}_0) \quad (78)$$

for $\mathbf{r} \in \mathbb{R}^3 \setminus (B_+ \cup B_-)$ and some coefficients $c_{l,m}^\pm$. Then, inside the spheres, the potential $V(\mathbf{r})$ for $\mathbf{r} \in B_\pm$ is given by

$$V(\mathbf{r}) = \sum_{l=0}^{\infty} \sum_{m=-l}^l \frac{f_{lm}^+}{R^{2l+1}} \mathcal{Z}_{lm}(\mathbf{r} - \mathbf{r}_0) + \frac{f_{lm}^-}{R^{2l+1}} \mathcal{Z}_{lm}(\mathbf{r} + \mathbf{r}_0) \quad (79)$$

Proof. The conclusion immediately follows from the definition of the solid harmonics \mathcal{Y}_{lm} and \mathcal{Z}_{lm} . \square

6.2. From TO to multipole expansion. When we apply the hybrid numerical scheme, we need to convert a TO solution into a multipole expansion.

Let us consider the following general potential W_\pm in the form of TO solution:

$$W_\pm(\mathbf{r}) = \sum_{n=0}^{\infty} \sum_{m=-n}^n a_{n,\pm}^m \mathcal{M}_{n,\pm}^m(\mathbf{r}) \quad (80)$$

for some coefficients $a_{n,\pm}^m$. We want to convert the potential W_\pm into a multipole expansion form as follows:

$$W_\pm(\mathbf{r}) = \begin{cases} \sum_{l=0}^{\infty} \sum_{m=-n}^n c_{lm}^\pm \mathcal{Y}_{l,m}(\mathbf{r} \mp \mathbf{r}_0), & \mathbf{r} \in \mathbb{R}^3 \setminus B_\pm \\ \sum_{l=0}^{\infty} \sum_{m=-n}^n d_{lm}^\pm \mathcal{Z}_{l,m}(\mathbf{r} \mp \mathbf{r}_0), & \mathbf{r} \in B_\pm \end{cases} \quad (81)$$

where coefficients c_{lm}^\pm and d_{lm}^\pm are to be determined.

We derive explicit formulas for $c_{l,m}^\pm$ and $d_{l,m}^\pm$ in the following theorem. Its proof is given at the end of this section.

Theorem 8. (Conversion of TO solution into multipole expansion) The multipole coefficients $c_{l,m}^\pm$ are represented in terms of TO coefficients $a_{n,\pm}^m$ as follows:

$$\begin{cases} c_{lm}^\pm = 2\alpha R^{2l+1} \sum_{n=|m|}^{\infty} a_{n,\pm}^m g_n^m \mathcal{D}_{lm}^\pm[\lambda_n^m] \\ d_{lm}^\pm = 2\alpha \sum_{n=|m|}^{\infty} a_{n,\mp}^m e^{-(2n+1)s} g_n^m \mathcal{D}_{lm}^\pm[\lambda_n^m] \end{cases} \quad (82)$$

In view of equation (81), the total flux on the surface ∂B_\pm is given as

$$\int_{\partial B_\pm} \frac{\partial W_\pm}{\partial \mathbf{n}} dS = 4\pi c_{0,0}^\pm, \quad \int_{\partial B_\pm} \frac{\partial W_\mp}{\partial \mathbf{n}} dS = 0 \quad (83)$$

So, we have the following flux formula from the above theorem.

Theorem 9. (Total flux formula) Let W_\pm be the potential given as equation (80). Then the total flux on the surface ∂B_\pm is

$$\int_{\partial B_\pm} \frac{\partial W_\pm}{\partial \mathbf{n}} dS = 8\pi\alpha \sum_{n=0}^{\infty} a_{n,\pm}^0, \quad \int_{\partial B_\pm} \frac{\partial W_\mp}{\partial \mathbf{n}} dS = 0 \quad (84)$$

6.3. Coordinate transformation for multipole expansion: translation and rotation. To apply the multipole expansion method, we need to represent a multipole source in a translated or rotated coordinate. It was shown that the following identities hold.¹

Translation:

We have

$$\begin{aligned} \mathcal{Y}_{lm}(\mathbf{r} - \mathbf{r}') &= \sum_{a=0}^{\infty} \sum_{b=-a}^a w_m w_b w_{m-b} \\ &\quad \times N_{lmab} (-1)^{l+a} Z_{ab}(\mathbf{r}_<) \mathcal{Y}_{l+a, m-b}(\mathbf{r}_>) \end{aligned} \quad (85)$$

where $\mathbf{r}_<$ is the smaller (in magnitude) of \mathbf{r} and \mathbf{r}' and $\mathbf{r}_>$ is the larger.

Rotation:

Suppose that the coordinate axes are rotated through Euler angle α, β, γ . The point (θ, ϕ) becomes $(\tilde{\theta}, \tilde{\phi})$. The following result holds:

$$Y_{lm}(\theta, \phi) = \sum_{M=-l}^l w_m w_M D_{mM}^{(l)}(\alpha, \beta, \gamma) Y_{lM}(\tilde{\theta}, \tilde{\phi}) \quad (86)$$

where

$$D_{mM}^{(l)}(\alpha, \beta, \gamma) = e^{-i\alpha + M\gamma} d_{mM}^l(\beta) \quad (87)$$

and

$$\begin{aligned} d_{mM}^l(\beta) &= \cos(\beta/2)^{2l+m-M} \sin(\beta/2)^{M-m} \\ &\quad \times \sum_t \sqrt{\binom{l+m}{t} \binom{l-M}{t} \binom{l+M}{l+m-t} \binom{l-m}{l-M-t}} \\ &\quad \times (-1)^t \tan(\beta/2)^{2t} \end{aligned} \quad (88)$$

The summation in t is carried over $\max(0, m-M) \leq t \leq \min(l+m, l-M)$.

6.4. Proof of Theorem 8. Let σ_{\pm} be the charge density on the surface ∂B_{\pm} , respectively. Now let us decompose σ_{\pm} using the spherical harmonics $Y_l^m(\theta_{\pm}, \phi_{\pm})$, where $(r_{\pm}, \theta, \pm, \phi_{\pm})$ are the spherical coordinates for $\mathbf{r} \mp \mathbf{r}_0$, respectively. Let us write σ_{\pm} as

$$\sigma_{\pm} = \sum_{l=0}^{\infty} \sum_{m=-l}^l \sigma_{lm}^{\pm} Y_{lm}(\theta_{\pm}, \phi_{\pm}) \quad (89)$$

Here, σ_{lm}^{\pm} can be determined using the orthogonality of the spherical harmonics as follows:

$$\sigma_{lm}^{\pm} = \frac{2l+1}{4\pi} \frac{1}{R^2} \int_{\partial B_{\pm}} \sigma_{\pm} \overline{Y_{lm}}(\theta_{\pm}, \phi_{\pm}) dS \quad (90)$$

To calculate the right-hand side of (90), we need to express σ_{\pm} and $Y_{lm}(\theta_{\pm}, \phi_{\pm})$ in terms of TO harmonics $Y_n^m(\eta, \varphi)$.

First, let us consider σ_{\pm} . Let 'ext'(or 'int') denote the limit from the outside (or inside) the sphere, respectively. It is well-known that the electric field $\mathbf{E} = -\nabla W$ satisfies the following boundary condition on ∂B_{\pm} :

$$\mathbf{E} \cdot \mathbf{n}|_{ext} - \mathbf{E} \cdot \mathbf{n}|_{int} = \sigma_{\pm}, \quad \text{on } \partial B_{\pm} \quad (91)$$

where \mathbf{n} is the outward unit normal vector to ∂B_{\pm} . To use the above condition, we need an explicit expression for W_{\pm} in the region inside the spheres B_{\pm} , respectively. From Theorem 6, we have, for $\mathbf{r} \in B_{\pm}$,

$$W_{\pm}(\mathbf{r}) = \sum_{n=0}^{\infty} \sum_{m=-n}^n a_{n,\pm}^m e^{(2n+1)s} \mathcal{M}_{n,\mp}^m(\mathbf{r}) \quad (92)$$

respectively. So, by using equation (7), we obtain

$$\begin{aligned} \sigma_{\pm} &= -\frac{\partial W}{\partial \mathbf{n}} \Big|_{\partial B_{\pm}}^{ext} + \frac{\partial W}{\partial \mathbf{n}} \Big|_{\partial B_{\pm}}^{int} \\ &= (2\alpha)^{1/2} [J(\eta)]^{-3/2} \\ &\quad \times \sum_{n,m} a_{n,\pm}^m (2n+1) e^{(n+\frac{1}{2})s} Y_n^m(\eta, \varphi) \end{aligned} \quad (93)$$

where $J(\eta)$ is defined by

$$J(\eta) = \frac{\alpha}{\cosh s - \cos \eta} \quad (94)$$

Next, let us consider $Y_n^m(\theta_{\pm}, \phi_{\pm})$. From equation (34) and Lemma 4, we have for $\mathbf{r} \in \partial B_{\pm}$,

$$\begin{aligned} Y_l^m(\theta_{\pm}, \varphi_{\pm}) &= R^{l+1} \mathcal{Y}_{l,m}(\mathbf{r} \mp \mathbf{r}_0) \\ &= R^{l+1} \mathcal{D}_{lm}^{\pm} [\mathcal{Y}_{|m|,m}(\mathbf{r} \mp \mathbf{z}_0)] \\ &= R^{l+1} (2\alpha)^{1/2} [J(\eta)]^{-1/2} \\ &\quad \times \sum_{n=0}^{\infty} g_n^m \mathcal{D}_{lm}^{\pm} [\lambda_n^m] e^{-(n+1/2)s} Y_n^m(\eta, \varphi) \end{aligned} \quad (95)$$

Now, we are ready to compute σ_{lm}^{\pm} . By substituting equations (93) and (95) into equation (90), we obtain

$$\begin{aligned} \sigma_{lm}^{\pm} &= \frac{2l+1}{4\pi} \frac{1}{R^2} \int_0^{2\pi} \int_0^{\pi} \sigma_{\pm} \overline{Y_{lm}} [J(\eta)]^2 \sin \eta d\eta d\varphi \\ &= (2l+1) 2\alpha R^{l-1} \sum_{n=|m|}^{\infty} a_{n,\pm}^m g_n^m \mathcal{D}_{lm}^{\pm} [\lambda_n^m] \end{aligned} \quad (96)$$

It is easy to check that the potential generated by the charge densities $\sigma_{\pm} = \sum \sigma_{lm}^{\pm} Y_{lm}$ is given as follows: for $\mathbf{r} \in \mathbb{R}^3 \setminus (B_+ \cup B_-)$,

$$W_{\pm}(\mathbf{r}) = \sum_{l,m} \sigma_{lm}^{\pm} \frac{R^{l+2}}{2l+1} \mathcal{Y}_{lm}(\mathbf{r} \mp \mathbf{r}_0) \quad (97)$$

By comparing the above expression and equation (81), we immediately arrive at

$$c_{lm}^{\pm} = \sigma_{lm}^{\pm} \frac{R^{l+2}}{2l+1} \quad (98)$$

Then, the formula for c_{lm}^{\pm} follows from equation (96). For the case of d_{lm}^{\pm} , it can be proved in a similar way. \square

REFERENCES

- ¹ Poladian, L. Effective Transport and Optical Properties of Composite Materials. Ph.D. thesis. (University of Sydney, 1990).
- ² Poladian, L. General theory of electrical images in sphere pairs. *Q. J. Mech. Appl. Math.* **41**, 395–417 (1988).
- ³ Poladian, L. Asymptotic behaviour of the effective dielectric constants of composite materials. *Proc. Roy. Soc. A* **426**, 343–359 (1988).
- ⁴ Goyette, A. & Navon, A. Two dielectric spheres in an electric field. *Phys. Rev. B* **13**, 4320–4327 (1976).
- ⁵ Cheng, H. & Greengard, L. A method of images for the evaluation of electrostatic fields in systems of closely spaced conducting cylinders. *SIAM J. Appl. Math.* **58**, 121–141 (1998).
- ⁶ Cheng, H. On the method of images for systems of closely spaced conducting spheres. *SIAM J. Appl. Math.* **61**, 1324–1337 (2000).